




Article

MASTER Real-Time Multi-Message Observations of High Energy Phenomena

Vladimir M. Lipunov ^{1,2,*} , Viktor G. Kornilov ^{1,2}, Kirill Zhirkov ¹, Artem Kuznetsov ², Evgenii Gorbovskoy ², Nikolai M. Budnev ³ , David A. H. Buckley ⁴, Rafael Rebolo Lopez ⁵, Miquel Serra-Ricart ⁵ , Carlos Francile ^{6,7}, Nataly Tyurina ², Oleg Gress ^{2,3}, Pavel Balanutsa ², Gleb Antipov ², Daniil Vlasenko ^{1,2}, Vladislav Topolev ^{1,2}, Aristarkh Chasovnikov ^{1,2}, Sergei I. Svertilov ^{1,8}, Ricardo Podesta ^{6,7}, Federico Podesta ^{6,7}, Ekaterina Minkina ², Andrei G. Tlatov ⁹, Vladimir V. Yurkov ¹⁰, Alexandre Gabovich ¹⁰, Olga Ershova ³, Viktor Senik ² and Dmitrii Kuvshinov ^{1,2}

- ¹ Physics Department, Lomonosov Moscow State University, Leninskie Gory, GSP-1, Moscow 119991, Russia; victor@sai.msu.ru (V.G.K.); zhirkov@sai.msu.ru (K.Z.); vlasenko@sai.msu.ru (D.V.); topolev@sai.msu.ru (V.T.); chasovnikov@sai.msu.ru (A.C.); sis@coronas.ru (S.I.S.); kuvshinov@sai.msu.ru (D.K.)
- ² SAI, Lomonosov Moscow State University, Universitetsky Pr., 13, Moscow 119234, Russia; akuznetsov@sai.msu.ru (A.K.); gorbovskoy@sai.msu.ru (E.G.); tiurina@sai.msu.ru (N.T.); mr.grol08@mail.ru or gress@sai.msu.ru (O.G.); balanutsa@sai.msu.ru (P.B.); gantipov@gmail.com (G.A.); minkina@sai.msu.ru (E.M.); senik@sai.msu.ru (V.S.)
- ³ Applied Physics Institute, Irkutsk State University, 20 Gagarin Blvd, Irkutsk 664003, Russia; nbudnev@api.isu.ru (N.M.B.); ershova@sai.msu.ru (O.E.)
- ⁴ South African Astronomical Observatory, P.O. Box 9, Observatory, Cape Town 7935, South Africa; dah.buckley@sao.ac.za
- ⁵ Instituto de Astrofísica de Canarias, Via Lactea, s/n, E38205 La Laguna, Spain; rrl@iac.es (R.R.L.); mserra@iac.es (M.S.-R.)
- ⁶ Observatorio Astronómico Félix Aguilar (OFA), Avda Benavides 8175, Rivadavia, El Leonsito, San Juan 5400, Argentina; cfrancile@unsj-cuim.edu.ar (C.F.); ricpod@hotmail.com (R.P.); karmaguitar@hotmail.com (F.P.)
- ⁷ Facultad de Ciencias Exactas Físicas y Naturales, San Juan National University, Casilla de Correo 49, San Juan 5400, Argentina
- ⁸ Skobeltsyn Institute of Nuclear Physics, Lomonosov Moscow State University, Moscow 119234, Russia
- ⁹ Kislovodsk Solar Station of the Pulkovo Observatory, P.O. Box 45, ul. Gagarina 100, Kislovodsk 357700, Russia; tlatov@mail.ru
- ¹⁰ Department of Physics and Mathematics, Blagoveschensk State Pedagogical University, Lenin Str., 104, Blagoveschensk 675000, Russia; yurkov@sai.msu.ru (V.V.Y.); gabovich@sai.msu.ru (A.G.)
- * Correspondence: lipunov2007@gmail.com or lipunov@sai.msu.ru



Citation: Lipunov, V.M.; Kornilov, V.G.; Zhirkov, K.; Kuznetsov, A.; Gorbovskoy, E.; Budnev, N.M.; Buckley, D.A.H.; Lopez, R.R.; Serra-Ricart, M.; Francile, C.; et al. MASTER Real-Time Multi-Message Observations of High Energy Phenomena. *Universe* **2022**, *8*, 271. <https://doi.org/10.3390/universe8050271>

Academic Editors: Chitta Ranjan Das, Alexander S. Barabash and Vitalii A. Okorokov

Received: 1 April 2022

Accepted: 22 April 2022

Published: 5 May 2022

Publisher's Note: MDPI stays neutral with regard to jurisdictional claims in published maps and institutional affiliations.



Copyright: © 2022 by the authors. Licensee MDPI, Basel, Switzerland. This article is an open access article distributed under the terms and conditions of the Creative Commons Attribution (CC BY) license (<https://creativecommons.org/licenses/by/4.0/>).

Abstract: This review considers synchronous and follow-up MASTER Global Robotic Net optical observations of high energy astrophysical phenomena such as fast radio bursts (FRB), gamma-ray bursts (including prompt optical emission polarization discovery), gravitational-wave events, detected by LIGO/VIRGO (including GW170817 and independent Kilonova discovery), high energy neutrino sources (including the detection of IC-170922A progenitor) and others. We report on the first large optical monitoring campaign of the closest at that moment radio burster FRB 180916.J0158+65 simultaneously with a radio burst. We obtained synchronous limits on the optical flux of the FRB 180916.J0158+65 and FRB 200428 (soft gamma repeater SGR 1935+2154) (The CHIME/FRB Collaboration, *Nature* 2020, 587) at 155093 MASTER images with the total exposure time equal to 2,705,058 s, i.e., 31.3 days. It follows from these synchronous limitations that the ratio of the energies released in the optical and radio ranges does not exceed 4×10^5 . Our optical monitoring covered a total of 6 weeks. On 28 April 2020, MASTER automatically following up on a Swift alert began to observe the galactic soft gamma repeater SGR 1935+2154 experienced another flare. On the same day, radio telescopes detected a short radio burst FRB 200428 and MASTER-Tavrida telescope determined the best prompt optical limit of FRB/SGR 1935+2154. Our optical limit shows that X-ray and radio emissions are not explained by a single power-law spectrum. In the course of our observations, using special methods, we found a faint extended afterglow in the FRB 180916.J0158+65 direction associated with the extended emission of the host galaxy.

Keywords: gamma-ray bursts; FRB; neutrino; gravitational waves; prompt; afterglow emission; multi-wavelength; multi-messenger observations; black holes; neutron stars; binary merging

1. Introduction

Extreme phenomena such as gravitational wave events (GW), fast radio bursts (FRB [1–4]), gamma-ray bursts (GRB [5–8]) and the generation of neutrinos of high and ultrahigh energies have been studied very intensively in recent years [1–13], but there still exist many problems, where the effective ways of solving these problems involve using multi-channel and multi-wavelength observations.

MASTER Global Robotic Net [5–8] was designed to investigate the error-fields of such high energy astrophysics phenomena, to discover their optical counterparts and to investigate their features. With the discovery of gamma-ray bursts [14,15], it became clear that our Universe contains ultra-fast highly energetic phenomena caused by the catastrophic collapse of a massive star. These transients shine so brightly that they are detectable at the other edge of the Universe, even by small fully robotic telescopes. The discovery of gravitational waves by LIGO experiment offers a prospect of exploring the Universe in a fundamentally new range [16–21]. The experience of optical support for the first observations shows that optical localization of GW events is an extremely difficult task for several reasons. First, most of the detected events were associated with black-hole mergers (in full agreement with prediction, calculated at Scenario Machine [22–24]). The second is the short time that such extreme objects are available for observers in any electromagnetic range. The third is large error-boxes of all GW events, which should be inspected in short time to discover such short live objects in electromagnetic range and to obtain its energy distribution to understand its nature. MASTER worked intensively on such events using full robotic observations, which let us automatically inspect error-fields by own central planner, similarly to how it was done with IceCube-170922 event [25], LIGO/Virgo GW events [26], and GRBs [8,27–34]. MASTER robotic software means fully automatic ephemeris, meteorological and hardware control, calibration images at sunset/sunrise, survey with wide-field images (2×4 square degrees) primary reduction and full identification of all sources at images no longer than 1–2 min after CCD readout, new optical transients (OTs) detection and analysis of its light curve, short reports for further investigations, and central planner with distribution of the areas of observation between neighboring MASTER observatories.

Gamma-ray bursts, high energy neutrinos sources, sources of gravitational waves and radio bursters can be related events.

MASTER main scientific results in these high energy astrophysics phenomena research are the following.

- (1) The discovery of significant and variable linear polarization during the prompt optical flash of GRB 160625B [27].
- (2) The discovery of gamma-ray bursts (GRB) Smooth Optical Self-similar Emission—the new type of calibration for GRB, in which some of their class can be marked and share a common behavior. We named this behavior SOS-similar Emission and identify these subclasses of GRBs with optical light curves described by a universal scaling function [28].
- (3) Independent optical detection of the first LIGO/Virgo Neutron Star Binary Merger GW170817-Kilonova MASTER OTJ130948.10-232253.3/SSS17a [17,21] and the first in history gravitational-wave standard siren measurement of the Hubble constant with LIGO/Virgo collaboration [26].
- (4) The largest input in the optical support of LIGO/Virgo GW150914 event [16,18–20].
- (5) The detection of a strong evidence for high energy neutrino progenitor of the neutrino event IceCube-170922A [25].

- (6) The discovery of GRB 161017A optical counterpart by MASTER and prompt follow-up multi-wavelength observations of this GRB by Lomonosov space observatory of MSU and MASTER Global Robotic Net [8].
- (7) The discovery of several dozens of optical counterparts of gamma-ray bursts, including the nearest GRB 180728A, the brightest GRB 190530A, and investigation of several thousands of GRB error-fields, detected by Fermi, Swift, Konus-Wind, Lomonosov, MAXI, Integral, HETE [5–8,27–34].
- (8) MASTER alert and follow-up observations of hundreds high energy neutrino error-boxes, triggered by IceCube, ANTARES detectors including the largest input to optical support of an IceCube multiplet in 2016y. -triplet IC160217 [35,36].
- (9) The discovery, photometry, hydrodynamics, and evolution scenario of luminous red nova MASTER OT J004207.99+405501.1/M31LRN2015 [37].
- (10) The discovery of an unusual bright eclipsing binary with the longest known period: MASTER OT J095310.04+335352.8/TYC 2505-672-1 [38].
- (11) The longest light curve (13.5 h of observations, 1124 data set), modeling and shape detection of Asteroid NEA 2015 TB145 [39], and observations of Near-Earth Optical Transients with the MASTER-Shok at Lomonosov Space Observatory [40,41].

It confirms effectiveness of MASTER alert, inspect and survey observations up to 20 m. In this paper, we present in detail the results of the FRB investigations.

2. FRB Observation

In the radio range, short-lived transients were not discovered until the beginning of the 21st century. It was only in 2007 that radio astronomers analyzing archival observations of the Parkes Radio Telescope first encountered fast transients [42,43]. More than 500 such sources have since been discovered.

The phenomenon of fast millisecond radio bursts (FRB) was predicted as a peculiar and very short “reincarnation” of a binary system consisting of old inactive magnetic neutron stars during their merging [44]. Such one-time radio bursts, accompanied by the death of the object itself [45], may occur when two neutron stars merge [17,21]. Gravitational waves from two neutron star binary mergers have been observed by LIGO/Virgo [17,46], although none yet in coincidence with FRBs. However, as it always happens, the phenomenon turns out to be complicated. It seems that we are dealing with at least two different classes of sources: unique bursts that never repeat and repeating (FRB repeaters [1–4]).

Some of the leading hypotheses for repeating flares involve the activity of extremely powerful magnetic neutron stars—magnetars [47–50]. Moreover, it is possible that such magnetars can be formed during or after the merger of neutron stars. However, so far, no optical telescope has been able to detect the optical glow from an FRB [51]. The original aim of our research was investigating one of the 22 known repeating FRBs. FRB 180916.J0158+65 has been recently localized with a pinpoint radio astronomical accuracy [52]. Moreover, after the detection of about three dozen radio bursts, it turned out that the activity of the FRB seems to repeat with a period of 16.35 ± 0.18 days [53].

It is obvious that the closer an FRB is, the more significant even the upper limit set by us will be. It was this thought that led to our optical monitoring. However, in the middle of our monitoring of FRB 180916.J0158+65, our research object ceased to be the closest FRB. It was found to be the galactic soft gamma repeater SGR 1935+2154, known since 2014 [54], located in the center of the supernova remnant G57.2+0.8 at a distance of ≈ 10 kpc from the Earth [55–58]. Since 2014, the source has been activating sporadically [59], and after a 3.24 s period was detected, it became clear that we are dealing with a magnetar possessing a magnetic field of $\approx 2 \times 10^{14}$ G [60]. On 27 April 2020 at 18:26:20 UT, the Swift Burst Alert Telescope (BAT) triggered and located a burst from the soft gamma repeater SGR 1935+2154 (trigger # 968211, [61–63]. The next day, the awakened gamma repeater emitted about a hundred pulses, one of which coincided with an outstanding bright radio burst, unlike any other radio burst from FRBs, with an accuracy of a millisecond. Thus, for the first time in

history, radio burster repeaters were discovered in a completely different spectral range, bar the long-known type of soft gamma repeater sources.

Thus, from 28 April 2020 to 5 May, our telescopes began to simultaneously trigger on the Swift and INTEGRAL gamma telescope alerts adding to the observations of the first FRB discovered in our Galaxy, SGR 1935+2154.

2.1. Methods

The main instrument of our research is the MASTER Global Robotic Telescopes Network [5,6] that consists now of 9 twin telescopes (MASTER Global Robotic Telescopes are marked by Russian flags at Figure 1): MASTER-Amur, -Tunka, -Ural, -Kislovodsk, -Tavrida (Moscow, Russia), -SAAO (Cape Town, South Africa), -IAC (Santa Cruz de Tenerife, Tenerife, Spain), -OFA (San Juan, Argentina), -OAGH (Cananea, Mexico, built in December 2021). This is a network of fully robotic twin wide-field (40 cm MASTER-II, 2×4 sq.deg., Figure 2) and twin very wide-field (MASTER-VWF cameras, 2×384 sq.deg.), colored (BVRI+polarization), fast (30 deg/s) telescopes with identical scientific equipment [5–7,64], and with our own real-time auto-detection system [5,6] distributed all over the Earth. Each MASTER site is equipped with two wide-field ($F/D = 2.5$) mirror-lens telescopes MASTER II with a diameter of $D = 40$ cm and two fast ultra-wide-field cameras MASTER-VWFC. Full frame CCD Apogee AltaU16 cameras (4096×4096 pixels, CCD with a scale of $1.85''/\text{pixels}$) provide a wide field of view (4 square degrees). In addition, two Prosilica fast very wide-field cameras (MASTER-VWFC) are installed on the same mount, which work without wasting virtually no time for reading. Prosilica cameras (4008×2672 pixels) with Nikkor 85 mm $f/1.4$ lens provide almost continuous exposures up to 3 frames per second at 384 square degrees). Each MASTER tube includes a robotic photometer equipped with two broadband filters (BVRI), one linear polarizer, and the so-called clear filter—a transparent glass plate with an optical thickness that compensates for the displacement of the focal plane when changing filters quickly (more details about the features of the MASTER equipment, see [5–7,64,65]).

We have been working to discover possible sources of FRB and to observe their error-boxes since 2014 [45,66–76]. It is possible if one has a fully robotic telescope network with a full real-time reduction software that identifies all optical sources at images to discover new optical transients (OT) just after a CCD readout, that is additionally distributed all over the Earth to exclude day/night/rain factors, as our network does [5,6]. All presented observations were carried out on 6 twin MASTER telescopes of MASTER network (Figure 1).

2.2. MASTER Instruments for Observations

We used the Apogee Alta U16 CCD cameras as main instruments, which are based on the Kodak-KAF16803 chip (widely used in astronomy). These cameras have a Pelletier cooling system (up to 40 degrees relative to the ambient temperature), were designed to operate in the optical range and, at their maximum, have an efficiency output of up to 70% at ~ 5800 Å. These cameras belong to classic CCD cameras and have a significant time for digitizing (reading) the image. So, a full frame without subframe and binning is read in 23 s. Installed on the MASTER-II robotic telescope, these cameras can acquire images with a limit of up to 21 m (unfiltered).

The Allied Vision GE4000 CCD camera is based on the Kodak KAI-11002 chip. The chamber is not cooled, it is designed for operation in the optical range, and has a maximum quantum efficiency of up to 50% at ~ 5000 Å. Due to special readout registers, the camera allows you to read and expose images at the same time. Thus, as a result, you can capture a “movie”, i.e., consecutive frames without time intervals. Due to the connection via a high-speed Ethernet interface, the camera is capable of delivering up to 3 frames per second. The camera is used in the ultra-wide-field channel of the MASTER-II telescope and in conjunction with wide-angle lenses allows one to have a large field of view ($FOV = 384$ square degrees).



Figure 1. Scheme of MASTER interaction with sites in Canada, Hawaii and New Mexico CHIME/FRB [1–4], Gemini North [52], VLA [77] to search FRB 180916.J0158+655 optical source. Observations of SGR/FRB 200428.J1935+2154 were carried out using alerts from the Gamma Center Network site at NASA. The physical map was taken from <http://observ.pereplet.ru/> (accessed on 1 March 2021); the stellar background was made by MASTER.

The mount provides a good slewing speed (up to 15–20 deg/s) as well as fast convergence and divergence of tubes. The latter option provides two different modes of operation for the telescope. The first is the sky survey mode. In this overview mode, the divergence of the tubes doubles the total field of view and, accordingly, the speed of view is also doubled. The second mode is an alert mode for target designations from other automatic installations, providing an error region with a radius of less than 1 degree. In the alert mode with small error-boxes, short-lived and rapidly changing events such as gamma-ray bursts and soft gamma repeaters (SGR) can be captured simultaneously in different spectral bands or in different polarization planes. These alerts usually come from NASA Dr. Barthelmy's Coordination Center [78,79] and are supplied by observatories such as Swift, INTEGRAL, Fermi-LAT, ANTARES, IceCube, Baksan, LIGO/Virgo, IceCube, etc.

There is another type of alert when the error-box is larger than the field of view of one tube. In this case, after fast (usually within 1 min after the event) guidance, the mode resembles our standard survey, but in certain fields of errors, sometimes reaching thousands of square degrees. Alert review mode is fully automatic and is called an inspection. In recent years, MASTER has been carrying out inspections of gamma-ray bursts (Fermi/GBM, IPN collaboration), sources of gravitational waves (LIGO/Virgo), and high energy neutrinos (ANTARES, IceCube, Baksan).

2.3. FRB 180916.J0158+65 and SGR/FRB 200428.J1935+2154 Different Observation Modes

To observe FRB 180916.J0158+65 and SGR/FRB 200428.J1935+2154, different observation modes were used. In the case of FRB 180916.J0158+65, the coordinates and approximate time were known, and it was a question of the possible detection of electromagnetic radiation in a completely different range-optical. Here we have applied an outstanding (about 40 days) monitoring of a single region in the sky with known coordinates. It would seem that the use of a system with a large field of view is not very effective for observing a point source with coordinates of radio astronomy accuracy. It would be much more efficient to use a large telescope with a small field of view and a fast radiation receiver. However, our planet does not have a unified network of such telescopes that could be used for several weeks. And this is exactly what is needed to capture an optical exposure at the moment of the flash. However, our system has such an advantage and is capable of long-term

monitoring of any object. In this case, the identity of telescopes and radiation receivers, and the possibility of long-term observations are on our side. In addition, over the course of monitoring, we found an opportunity to use the specific difference between our telescopes and other telescopes in the world, referring to the duality of MASTER telescopes (Figure 2).



Figure 2. MASTER-SAAO telescope-robot at the South African Astronomical Observatory (SAAO) near Sutherland. Typical design: two 400 mm tubes with a 2×4 square degrees field of view and two very wide-field view cameras (VWFC with FOV = 2×384 square degrees) at fast mount. The Figure was taken from <http://observ.pereplet.ru/> (accessed on 1 March 2021).

At first, we applied a standard search method—just continuous monitoring. We tried to find traces of two types of optical emission. Firstly, the emission is simultaneous with radio bursts. Secondly, a quasi-stationary optical component is possible.

We aimed to detect optical flares such as bursts in the radio range, i.e., durations of the order of one millisecond or longer (~ 1 s), as discussed in recent models of optical emission of magnetars [80]. Obviously, to detect such a short phenomenon requires the shortest possible exposure. After all, the constant sources in the star's frame and the noise of the night sky with an increase in exposure will dilute useful photons from an ultra-short flash. On the other hand, the minimum short exposures of our cameras in the region of 40–80 milliseconds are practically useless, since the frame reading time ~ 8 s. Therefore, this requires a special reduction mode (“CUTTING”, i.e., interleaving) frames. However, with a very small frame, we lose reference stars, and even with such exposures, the sensitivity decreases due to readout noise. Having two tubes and two CCD cameras, we chose the optimal mode without dead zones in time. Thus, the exposure was chosen so that the subject was shot by interleaving exposures on the two tubes. That is, while the image was read on the eastern tube, the exposure was being taken of the western one. It was similar to walk on a white board on a chessboard.

In addition, on two telescopes (MASTER-Amur and MASTER-Tunka), we put cameras for fast continuous shooting of the sky on one of the tubes. An analysis of the noise of fast cameras showed that the optimal shooting time should not be less than 2 s, due to the limitation of sensitivity by readout noise. On the other hand, with an increase in exposure of more than 5 s, we lost sensitivity due to the potentially short flash burst of the radio burster. Thus, we were able to shoot simultaneously with two telescopes the place of the radio burster with an ideal coincidence scheme with a higher temporal resolution on one of the tubes. Other MASTER telescopes at -Kislovodsk, -Tavrida, -IAC, and -South Africa sites were left as standard. This allowed us, if desired, to switch from the “checker” mode to simultaneous shooting with windows on full frame cameras.

When we finally captured a frame coincident with the radio burst and obtained only the upper limit of luminosity (see Figure 5), we began to look for a quasi-stationary glow from the FRB region. The usual method is that all frames are added together and thus increase the depth of the total image. In the case of random noise, the signal-to-noise ratio

grows as the root of the total exposure time or the root of the number of SNR frames $\sim\sqrt{N}$. However, in reality, this is not achieved due to the influence of non-Gaussian noise and systematic errors. In addition, optical emission can be flare-like (flickering). As a result, a new image processing method was used. We took only simultaneous frames received by both tubes almost simultaneously (less than 1 s). The most stable and numerous frames were those obtained with the MASTER-Kislovodsk telescope (Caucasus, Russia). We selected the best—there were more than 6000 pairs.

Further, from these thousands of pairs, we tried to find such events that simultaneously (that is, within 10 s exposure) in both tubes consist of three connected pixels, the signal on each should exceed noise as 1.5 sigma. In this case, for us, in general, the character of emission is not important. Even in the case of aperiodic or periodic pulses due to the coincidence circuit, the reliability of their detection increases sharply. So an experienced amateur astronomer looks at the Saturn for a long time trying to catch rare moments when the Cassini gap is visible.

Exposures were chosen so as to continuously observe the object, i.e., while frame is being read on the eastern tube, frame is being shot on the western. Since the minimum readout time of our CCD cameras can be 8 s, minimal exposure time was chosen to be 10 s. Results of the analysis of concurrences are shown in Table S1.

3. Statistical Substantiation of the Search for Weak Signal by Coincidence Methods for Double Telescopes

We will describe the idealized case and, gradually complicating the situation, we will come to a comparison with the data obtained with MASTER telescopes. Suppose that the probability distribution of the number of incoming photons obeys the Poisson distribution: $P(n) = \frac{\langle n \rangle^n}{n!} e^{-\langle n \rangle}$. It is usually used to describe incoming photons from a region of the sky, as well as for emitting objects [81]. Let us introduce additional parameters typical for CCD and consider the equation of the incoming signal and noise. η —quantum efficiency, D —effective diameter of the observing system, t —exposure time (signal lifetime), β —angular size of an extended object, $\langle n_s \rangle = \eta D^2 t f_s$ —the average number of counts, if the signal is set by a luminous object for a long time. For an extended object, the formula will be $\langle n_s \rangle = \eta D^2 t \beta^2 f_s$, same formula for sky background ($\langle n_b \rangle = \eta D^2 t \beta^2 f_b$ —background signal); only the surface brightness will differ in them. In these two cases (point and extended source), the distribution of the number of photons can be characterized by the Poisson distribution, therefore, one can easily obtain an expression for the signal variance $\sigma = \sqrt{n_s}$. However, due to the fact that we are considering FRB, which can emit impulsively and correlated, the number of samples can be described by a more complex distribution function, which in the most general case can be characterized a priori by a given mean and variance. It is easy to see that in the strong background approximation, only the average of the properties of the incoming radiation will be important. In what follows, we will consider an effect that occurs only for a very short radiation time, but so far, it is not important in our reasoning. We agree to consider that with all other constants corresponding to a certain system, for each exposure, on average, a constant value is accumulated: n_s^0 —for signal, n_b^0 —for background.

Let us consider direct addition of images. It would be equivalent to increasing the exposure time $\sim N$ (number of frames) $\langle n_\Sigma \rangle = N(n_s^0 + n_b^0)$.

Due to the properties of the Poisson distribution for the sum— $\sigma_\Sigma = \sqrt{\langle n_\Sigma \rangle}$. Even if we consider our source to be not Poisson, in the strong background approximation $\sigma_b \gg \sigma_s$, $\sigma_\Sigma \approx \sqrt{N} \sigma_b$. Expressing the total signal and finding the relative error (SNR): $N n_s^0 = \langle n_\Sigma \rangle - N n_b^0$.

$$\varepsilon_{N n_s^0} = \frac{\sqrt{\langle n_\Sigma \rangle + N n_b^0}}{N n_s^0}, \text{ which simplifies to the form—} \varepsilon_{N n_s^0} = \frac{\sqrt{2 N n_b^0}}{N n_s^0} \sim \sqrt{\frac{n_b^0}{N}} / n_s^0$$

Thus, with the addition of thousands of frames, a significantly smaller signal can be seen against the background of sky noise. On a good night, the sky background can reach 21.5 m—at a pixel size of 4 square seconds, this gives the background contribution to the

number of photon counts at the object level 20 m. Then, when exposing 6134×2 frames, you can capture an object with $\text{SNR} \approx 3$ to 24 m. It is important to estimate the number of photons arriving at the telescope, because one may encounter a situation when, on average, more than one photon may not come from the object during the observed period during the exposure. For a tube with a diameter of 40 cm and exposures in 10 s, from the object 20 m, only about 200 photons will come, and from the object 25 m, values will come, on average, a pair of light quanta, which, taking into account the quantum efficiency of the CCD and the readout errors, will most likely be impossible to distinguish from noise. These estimates can also be used to determine the characteristic probability of kurtosis, using the properties and definition of the Poisson distribution.

Unfortunately, such an idealized situation is far from true due to the fact that in addition to sky noise, there are contributions from CCD readout noise, as well as errors associated with distortion of the shape of the image of the desired object. All this increases the variance of the samples. Similarly, we introduce the value n_r^0 (may be less than 0, in contrast to the contribution of the source and the sky background), which will describe the effect of all other errors on the observed mean. This quantity will not be described by the Poisson distribution, therefore it is difficult to take it into account. Obviously, all these factors will strongly interfere with reaching the theoretical limit of 24 m due to the introduction of an additional term in the relative deviation of the calculated signal.

The presence of two tubes makes it possible to create a simple analogue of the coincidence scheme, which will significantly reduce the possibility of “accidental” identification of a phenomenon as an object, especially as this helps to deal with random cosmic particles and errors in the operation of CCD (Figure 3). Such a scheme was supposed to help automatically find the most reliable candidates that could be identified with FRB180916.J0158+65, but although many candidates were found, single pairs of frames did not allow us to reliably talk about the presence of a flash of optical radiation. We have proposed a simple statistical method for processing a large array of such candidates by comparing with a reliably empty (within the framework of observations), up to 23 m region near the observed place.

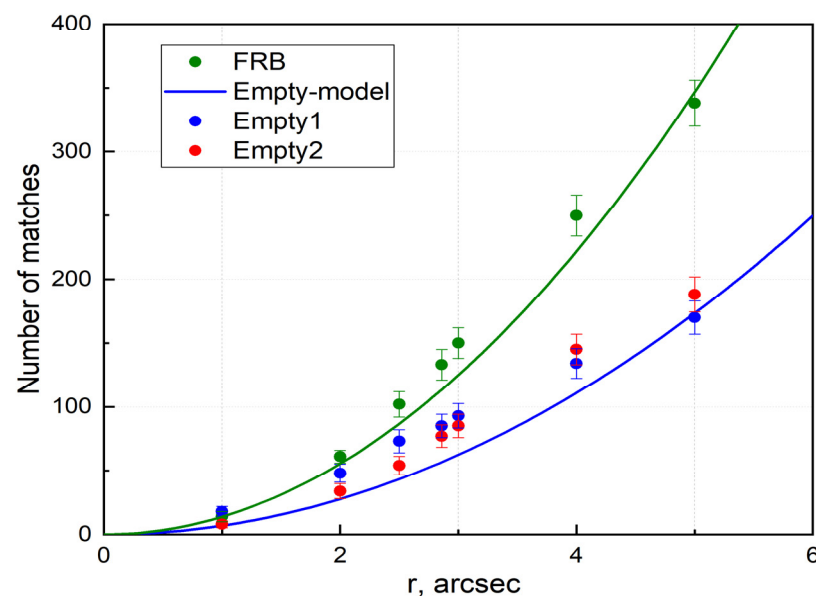


Figure 3. The dependence of the number of synchronous coincidences in both tubes at the level of 3 sigma on the radius of the circular analyzed region in angular units. Green dots show the area around the FRB 180916.J0158+65. Green and blue curves are expected theoretical results for an object and an empty place.

Consider a scheme that will count the number of synchronous elevations over the background for two tubes for a fixed area of the sky in N frames. The criterion for exceeding the background level will be the existence in our selected area of the sky of a

group of or more adjacent pixels, in each of which, the number of samples exceeds the average value by more than sigma. The probability of such an event for a randomly taken pixel can be obtained in the form: $P = p_0^2(C_4^4 p_0^4 + C_4^3 p_0^3(1 - p_0) + C_4^2 p_0^2(1 - p_0)^2)^2$, where $p_0 = p(x > \langle x \rangle + \sigma)$. This formula is obtained under the assumption that the errors in different tubes are independent. The nature of the distribution affects the value p_0 . By multiplying this expression by the area in pixels, you can get an estimate of the probability of finding a random criterion. As a first approximation, we can take p_0 similar for the normal distribution, which is taken equal to 0.158, then the mathematical expectation of the number of matches— $M(r) = PS_r N \approx 3.6 \times 10^{-4} S_r N$. r —search radius in pixels, S_r —number of pixels. The theoretical curve is superimposed on the observations made (green curve, Figure 3).

Small deviations of the graph for empty spaces from the theory can be explained by the inaccuracy in determining σ from observations and the deviation of some noise from the normal distribution. It is worth noting the strong influence of probability p_0 by the total number of matches $M \sim p_0^6(1 - p_0)^4$, which makes the scheme especially sensitive to the type of distribution (Figure 4).

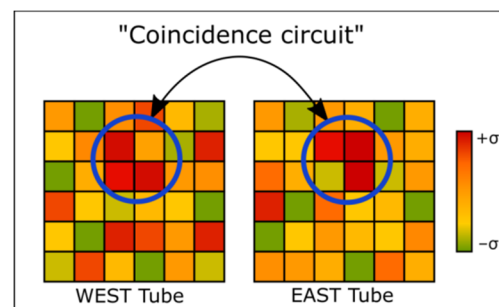


Figure 4. The illustration of the matching method for the twin-telescope MASTER. Only those events in a given direction are counted that simultaneously appear on both pipes in the form of three connected pixels, in each of which, the signal exceeds 1 sigma.

Now let us consider two options:

- (1) Extended object with $n_s^0 = k \sigma$ (creates a background in a large area, in every pixel). This case can be considered simply by considering the above formula with modified $p_0 = p(x + k\sigma > (\langle x \rangle + \sigma))$; for estimation, we can take a new value p_0 according to the normal distribution (for example, for $k \approx 0.15$; $p_0 \approx 0.184$), and the number of matches is of the order $p_0^6(1 - p_0)^4$. The final form of the dependence should be parabolic, but with a greater slope than the empty space. The curve at $k \approx 0.15$ is marked on the graph in purple. This k was specially selected for comparison with the resulting curve for the FRB site.
- (2) Point object with $n_s^0 = k \sigma$ and localization of the order of a couple of arcseconds (the center of the object can shift by distances of the order of the pixel size), similar to that described above, but the derivative undergoes a kink as soon as the coincidence radius is greater than the inaccuracy of determining the center of the object. Then there will be a parabolic growth as from an “empty” place.

The main conclusion drawn from the processing results is that the graphs obtained from the results of observations correspond more to a weak extended background object than to a point object. We calculate the S/N ratio in a straightforward way by comparing the error from the blank matches and the number of matches at the FRB site.

The error in determining the number of matches can be determined from the properties of the distribution of the number of samples (M), which obeys the binomial distribution, the variance of which is given by the well-known formula: $D(M) = \sigma^2 = S_r NP(1 - P)$. Thus, the error in measuring the ratio will be proportional to the root of the number of detected synchronous pairs (P is considered small).

Additionally, the search method has another good property with respect to direct addition—it is a decrease in blur caused by inaccurate positioning of the frame, even if the center of a point object wanders along the plane (due to a change in atmospheric refraction, a change in deformations of the optical system), the asymptotes for this method will be similar to a point object. In other words, by increasing the matching radius, we will have to arrive at the usual background parabola, but with the power of the point source raised accordingly.

In all the previous arguments, we did not touch upon the question of the dependence of the picture on the distribution of the arrival of quanta in time. An argument similar to the one described above will work here; the point signal is less smeared by the atmosphere, and therefore, most likely, it should be better registered.

The date was chosen by us since the next time of radio burster activity calculated by the ephemeris of the CHIME/FRB project was at the time of $\text{April } 10.4 \pm 2.6$.

In total, 155,093 images of the radio burster were obtained using 5 telescopes located in the northern hemisphere, and covered three periods of activity and partly phases of radio silence between them. Our telescopes are small in diameter, but they are twin and can shoot simultaneously in both tubes [5–7]. In the overwhelming majority of cases, we used two exposure times: 5 s (for fast cameras) and 10 s for full frame cameras. To process the observation results, we used a peculiar scheme of coincidences of the signal from both tubes.

4. FRB 180916.J0158+65 MONITORING

We tried several observing strategies for FRB 180916.J0158+65 before arriving at a final scheme. In the course of observations at two observatories, we replaced the slow (minimum 8 s readout) Apogee CCD from MASTER-II with the fast detectors (cameras) from our very wide-field channel (Prosilica GE4000 [5–7]); the field of view remains the same.

On 6 April 2020, the MASTER-Kislovodsk robot telescope (Caucasus, Russia) began optical monitoring of FRB 180916.J0158+65 at 20:36:16 UT (see also Figure 5). The subsequent schedule and observation regimes were determined by the ephemeris and local weather at the telescopes of the MASTER Global Network located in the northern hemisphere.

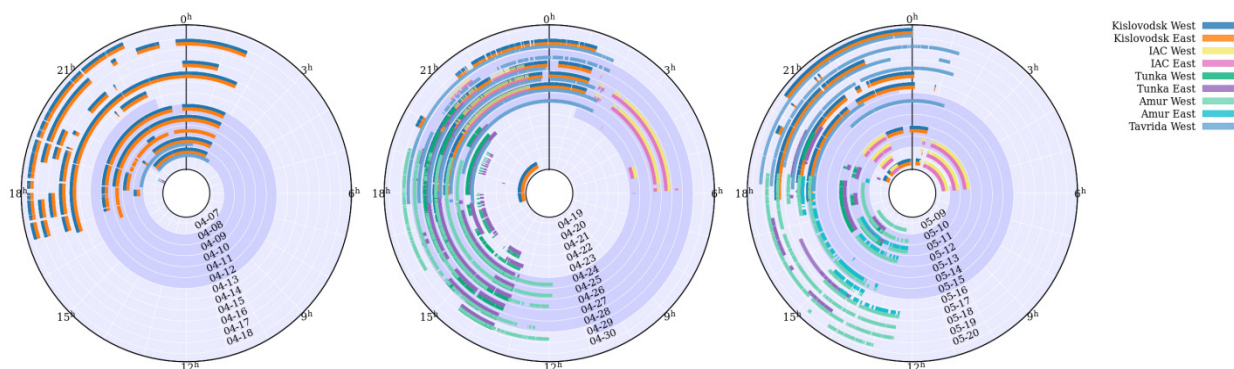


Figure 5. Schedule of synchronous observations of the FRB 180916.J0158+65 radio burst by five MASTER telescopes. The darker lilac rings show the moments of activity of the radio burster according to the ephemeris [53] © MASTER2022.

The date was chosen from the next time of FRB activity calculated by the ephemeris of the CHIME/FRB project, which was at the time of $\text{April } 10.4 \pm 2.6$. In total, 155,093 images of the radio burster were obtained (Figure 6), covering three periods of activity and partly, the quiescent periods, on the 5 telescopes located in the northern hemisphere. Our telescopes are small in diameter (0.4 m), but they are twin and can shoot simultaneously in both tubes each with potentially different filters [5–7]. In the overwhelming majority of cases, we used two exposure times: 5 s (for fast cameras) and 10 s for full frame cameras

(for Apogee cameras). To process the observation results, we used a peculiar scheme of coincidences of the signal from both tubes.

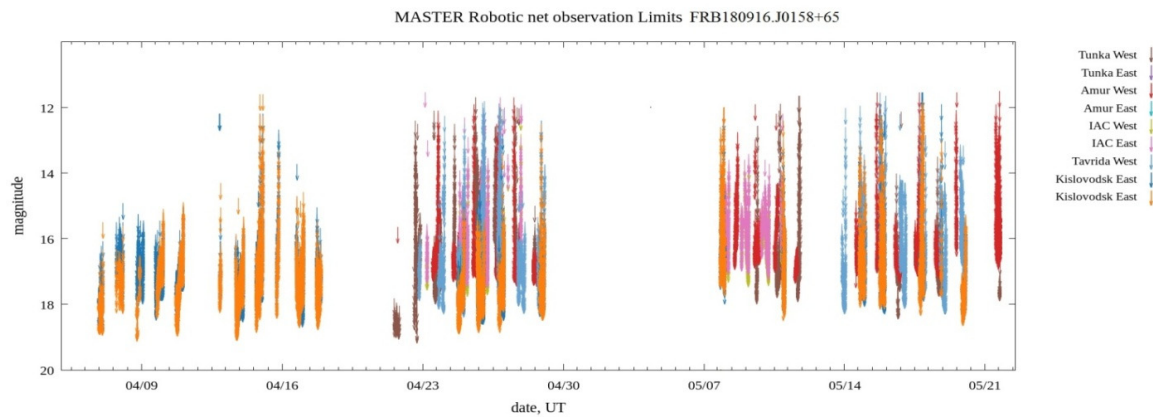


Figure 6. MASTER optical monitoring limit for FRB 180916.J0158+65 obtained at the 5 telescopes located in the northern hemisphere which covered 3 periods of activity and partly, the quiescent periods between them.

5. Results

5.1. The Detection of a Photon Excess on Two Telescopes Simultaneously near FRB 180916.J0158+65 Position

We assumed that optical emission could behave in a flash manner and that this activity increases during periods of FRB activity. If the duration of flashes is comparable to the duration of radio bursts, then they are measured in milliseconds, so it is difficult to expect source detection in each frame. A manual analysis of 10,000 images taken in April (see Table S1) led to the detection of a signal on about 40 frames near the coordinates of the FRB (Figure 7 and <http://master.sai.msu.ru/images/universe/figure7a.jpg> accessed on 28 April 2022), where we put the synthesized image of the host galaxy from Gemini open archive, that was published in Marcote et al. [52], and FRB place obtained by MASTER (the red round on the left Gemini square) and by Gemini).

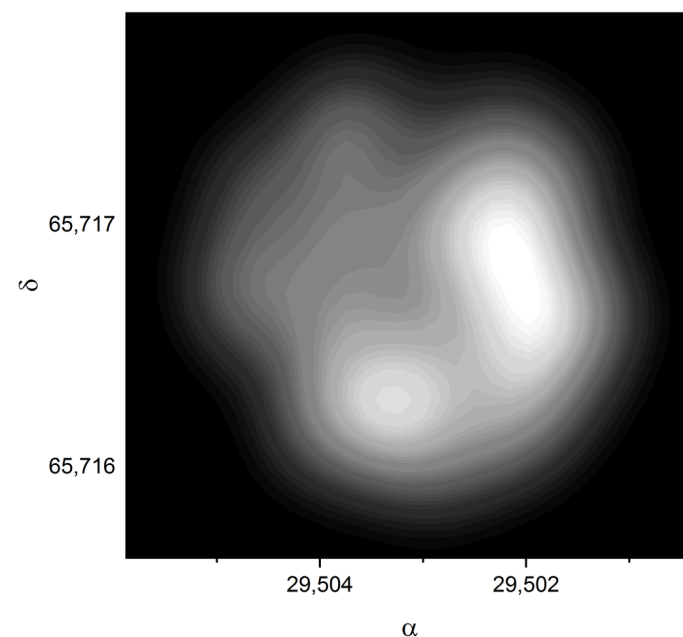


Figure 7. MASTER brightness distribution of the host galaxy region associated with FRB 180916.J0158+65.

Analysis of such a large number of images is not possible without automation of the process. Our standard processing was usually intended to search for transients on a small number of frames without an a priori knowledge of their positions. However, in this case, on our side was the knowledge of the coordinates of a possible source of optical emission. Knowing the coordinates and the presence of two simultaneous images has significantly increased the sensitivity (potential of detection) of our telescope and made it possible to find an optical counterpart. In fact, we collected on each frame at the position of the FRB all the pixels with a slight excess over the noise (see Section 2.1 and Supplementary Materials). Here we used the design features of our telescope (every MASTER observatory has twin MASTER 0.4 m telescopes) allowing us to observe an object simultaneously in both telescopes. At the same time, we accumulated cases when the signals were in both telescopes. We must note that the signal appeared in several percent of the simultaneous frames. Such a coincidence scheme made it possible to significantly reduce random spurious detections in individual telescopes and made it possible to isolate events at a level of more than $\text{SNR} \geq 3$. Obviously, with so many frames, random coincidences are still possible.

Among all the telescopes, the highest-quality simultaneous observations took place on the MASTER-Kislovodsk telescope. This is due to the high position of the object above the horizon and favorable weather conditions. On the MASTER-IAC telescope, the repeater was near the horizon and the frame limiting magnitudes were much worse than in the MASTER-Tavrida. On MASTER-Amur and MASTER-Tunka telescopes, both tubes worked but each tube had different types of cameras: full frame Apogee U16M cameras and fast Prosilica GE4000. The MASTER-Tavrida telescope, at the time, had only one operating tube.

Obviously, choosing the best images from thousands of images of different quality is possible only automatically. The accuracy of our standard automatic method is not great and is determined by many factors, including variable ones: the accuracy of catalogs, inhomogeneity of wide-field frames, variable transparency, and variability of the seeing). Therefore, we took advantage of the design features of the MASTER telescope that allow us to apply the coincidence scheme when the registration of quanta is counted only if it occurs in two parallel tubes simultaneously. Thus, we capture the rarest moments of transparency, calmness, and atmosphere. Experienced amateur astronomers know that in order to see the Cassini slit in the rings of Saturn from the city observatory, it takes several minutes, without stopping, to look through the eyepiece capturing the moment of calmness of the atmosphere for 0.1 s (constant time of the human eye). Something similar happens in our method.

To assess the accuracy of measurements, we collected similar information from a randomly selected empty place on those frames. We also made an analytical estimate of the number of random coincidences, which coincided well with the observed one. However, these “empty spaces” were not chosen entirely by chance. First, it was necessary to make sure that they did not have any objects up to magnitude 23 m. Secondly, they had to be outside the host galaxy, but close enough that the background heterogeneity would not be affected. Recall that we are dealing with a wide-field telescope. For the first empty place, we obtained the following coordinates: RA, Dec(2000) = 01 h 58 m 13.33 s, +65°46′27.8″. For the second one: RA, Dec(2000) = 01 h 57 m 57.25 s, +65°43′49.4″.

A total of 6134 pairs of simultaneous images were used. We selected events, if in each tube there were 3 pixels at the place of the FRB or the empty place with an excess of photons by 1 sigma in each telescope on the same frame. As a result, it turned out that in the place of FRB, the number of concurrences is 2.0 ± 0.25 times more than in deliberately random places. So, the excess of simultaneous samples on the FRB place was at the level of $\text{SNR} = 8$. This excess of photons is due to the optical emission of a weak extended source—a star formation region of the host galaxy. In the first case, the ratio of the number of concurrences around the FRB and the empty place should decrease with a decrease in the radius of the region around the radio burst. These data are in good agreement with the region visible in the Gemini image (Marcote et al. [52]). This is equivalent to ~25 m per 1 square arcsecond.

In September 2020, the images obtained with the Gemini telescope under the GN-2019A-DD-110 program (Marcote et al. [52]) became public. We used 450 s exposure-band image obtained by Gemini on 14 July 2019 14:26:29 UT. We performed circle aperture photometry of the galactic spot with a step of 1 pixel from the original image to estimate the contribution of the galaxy to the place where the search for candidates in the MASTER telescope was carried out. By increasing the aperture with a step of 1 pixel ($1.6''$), we obtained the curve of the growth of the galaxy brightness around the point with coordinates FRB180916.J0158+65. The results of our assessments are shown in Figure 8 (and Table S2 in Supplementary Materials).

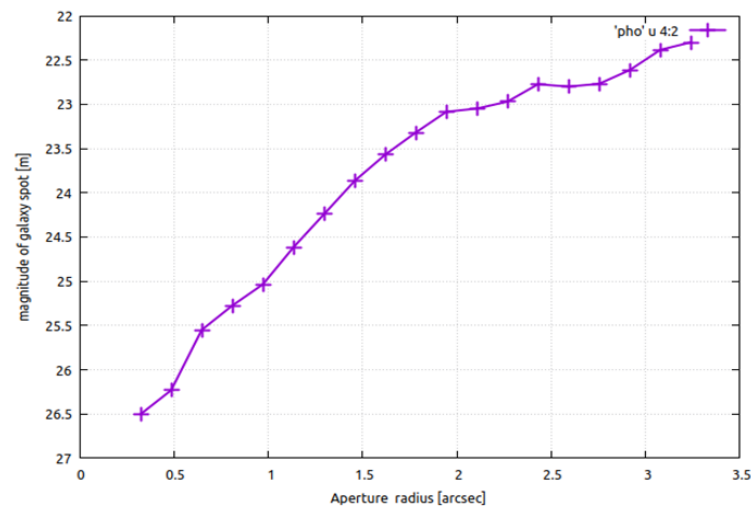


Figure 8. The brightness of the extended glow of the host galaxy (Table S2).

The average fluence normalized to the exposure of MASTER observations turned out to be $0.02 \text{ Jy}\cdot\text{ms}$. Accordingly, the average magnitude is 22.6 m . An analysis of the highest quality images of $\text{FWHM} \leq 2.5''$ limits magnitude to 22.9 m . This corresponds to a surface brightness of $25 \text{ magnitude per a square arcsecond}$. This matches the results of the Gemini image photometry (see Figure 8). Since our cameras are sensitive in a wide range of wavelengths with a large tail in the red region, we take an effective wavelength of 8000 Angstroms , in which the absorption is 1.4 m . Thus, the effective average fluence was $0.05 \text{ Jy}\cdot\text{ms}$.

5.2. Prompt Optical Observation of FRB 180916.J0158+65

On 23 April 2020 at 20:11:19.68 UTC (taking into account the dispersion of a radio signal), the VLA Karl Jansky radio telescope detected a radio burst from a repeating FRB 180916.J0158+65. The peak flux density of the burst was approximately 0.13 Jy over band ($1.36\text{--}2.0 \text{ GHz}$), and its temporal width was less than 10 ms . Accordingly, the radio fluence is $1.3 \text{ Jy}\cdot\text{ms}$. At this time, MASTER-Tunka robotic telescope located in Siberia continuously shot the radio burster and two images, on the eastern and western tubes (MASTER-II), turned out to be simultaneous with the radio burst. The cameras differed in their characteristics and in exposure time.

The first camera is a standard one, with an exposure time of 10 s . The frame, overlapping the moment of the burst, began at 20:11:11 UTC and ended at 20:11:21 UT. The magnitude limit for color $G-R = 1.14 \text{ m}$ is $m_{\text{lim}} = 17.7 \text{ m}$, for $G-R = 0.61$, it is $m_{\text{lim}} = 17.4 \text{ m}$. The second camera (fast Prosilica) imaged with an exposure time of 2 s . The coincident frame began at 20:11:19 UTC and ended at 20:11:21 UT. The magnitude limit for $G-R = 0.67 \text{ m}$ is $m_{\text{lim}} = 13.6 \text{ m}$, for $G-R = 1 \text{ m}$, it is $m_{\text{lim}} = 14.5 \text{ m}$. These colors are taken from PANSTARRS DR1, the magnitudes are from Gaia DR1. These limits are shown in Figure 9.

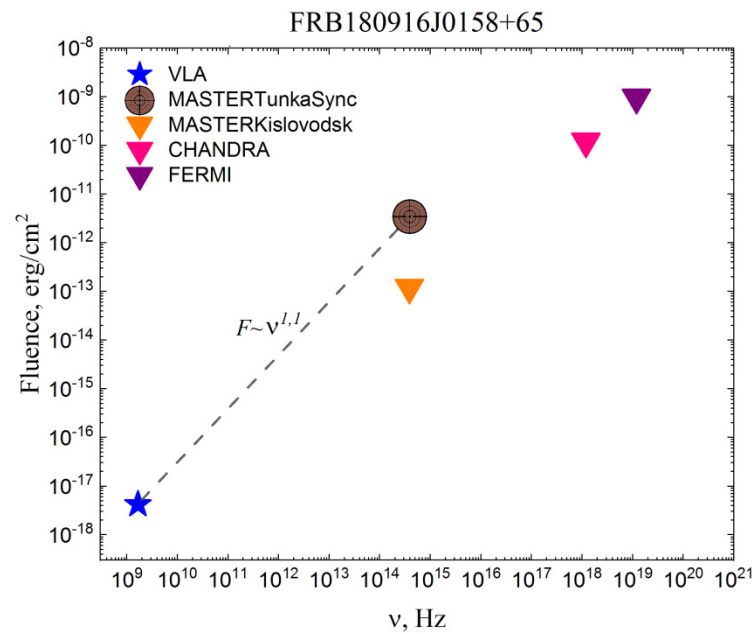


Figure 9. The dependence of the fluence in absolute units on the frequency of observation. This graph shows the limits and typical energies for FRB 180916. Fully filled dots represent FRB 180916. Stars—signal detection, triangles—upper limits. Azure Star—observation of FRB 180916 by the VLA radio telescope dated 23 April 2020 [77] ©VLA2020. MASTER-TunkaSync is synchronous observation of this burst with the MASTER-Tunka optical telescope. Chandra and Fermi GBM are non-simultaneous observations of FRB180916 in the ranges of 0.5–10 keV and 10–100 keV, respectively, Scholz et al. [82,83].

We did not detect the source at $\text{SNR} > 1.5$ in both simultaneous frames. Our full frame cameras are fairly red, so our effective wavelength of unfiltered images is at a wavelength of 8000 \AA . For this wavelength, effective absorption is equivalent to absorption in the I filter, which in this direction, is approximately 1.4 m. Our fast cameras are closer to the V filter where the absorption is 2 times stronger. Accordingly, our fluence limit for the slow Apogee camera of the first camera is $(1 \pm 0.1) \times 10^{-12} \text{ erg/cm}^2$, while for the Prosilica, it is $(3 \pm 1) \times 10^{-11} \text{ erg/cm}^2$. After taking into account absorption according to dust maps [84], our best fluence limit for simultaneous optical emission was found to be $1.7 \text{ Jy} \cdot \text{ms}$.

The FRB source is located in a fairly close galaxy [53] but it is invisible in our individual 10 s image. For cosmological parameters [85], $H_0 = 67.8 \text{ km/s/Mpc}$ (the Hubble constant), $\Omega_m = 0.308$, $\Omega_\Lambda = 0.692$ (the matter and vacuum density), and redshift $z = 0.0337 \pm 0.0002$ [52] corresponds to luminosity distance D_L equal to 152.8 Mpc. This corresponds to a limit of the total emitted optical energy of $2.6 \times 10^{44} \text{ erg}$. Comparison with simultaneous fluence in the radio range shows that:

$$\eta = \text{Fluence}_{\text{opt}} \cdot \nu_{\text{opt}} / \text{Fluence}_{\text{radio}} \cdot \nu_{\text{radio}} < 4 \times 10^5.$$

The obtained restriction on the simultaneous optical luminosity of the radio burster does not contradict the assessment in the framework of different scenarios of the generation of electromagnetic radiation of magnetars [48–50]. However, it should be emphasized that this limit differs by less than an order of magnitude from the predicted flux ratio in optics and radio in the model of interaction of relativistic particles with a supernova remnant [86]. It seems to us that it is necessary to continue attempts to detect radio bursters in different ranges and channels of information.

The optical flux recorded by us obtained outside the radio burst is much better and amounts to $1.3 \times 10^{40} \text{ erg/s}$ and is related to a birth-like star formation region in the heterogeneity of the host galaxy.

5.3. Prompt Optical Observation of Soft Gamma Repeater SGR/FRB 200428.J1935+2154

On 27 April 2020 at 18:26:20 UT, the Swift Burst Alert Telescope (BAT) was triggered by SGR 1935+2154 (trigger #968211). In terms of visibility and weather, the MASTER-Tavrida robot telescope was the first to respond [87]. MASTER-Tavrida had been observing it since 27 April 2020 21:57:38 UT to 28 April 2020 00:32:48 UT with unfiltered $m_{\text{lim}} = 20.0$ m. Observations began at altitude 26deg, and the sun altitude was -31 deg. Later, the telescopes of MASTER-SAAO (South Africa) and MASTER-IAC (Canary, Spain) were automatically joined to the observations.

On that first night, SGR 1935+2154 produced a whole forest of gamma-ray pulses, and MASTER's telescopes were able to simultaneously obtain limits on their prompt optical output of many gamma pulses. Figure 10 shows the limits for the energy fluences of optical radiation in the direction to the source, not corrected for absorption.

However, after the end of the night (sunrise) in the Canary Islands, observations were interrupted and resumed in the Russian Far East with the MASTER-Amur telescope after a few hours. The next alert from the SGR 1935+2154 was from the Integral satellite (trigger time 28 April 2020 14:34:24 UTC [10]. MASTER-Amur and MASTER-Tunka automatically started to observe it at 14:34:46 UT (22 s after trigger time) and at 28 April 2020 14:40:28 UTC respectively [87,88]. This gamma-ray burst alert originated from the same gamma-ray pulse, which was accompanied by a radio burst and was registered by the Integral detectors. Naturally, we weren't fast enough to detect emission simultaneously with the radio pulse [89]. Over the next week, mentioned telescopes continued monitoring, and covered two more bright soft gamma pulses and one weak radio pulse detected by the FAST telescope [90]. To account for absorption and recalculate our optical fluence limits, we used the derived hydrogen column densities. According to measurements in the soft X-ray range on devices, the best estimate is column density $N_{\text{H}} = 2.4 \times 10^{22} \text{ cm}^2$ [91]. This corresponds to absorption by interstellar dust on the order of 6.2 m in our red CCD cameras in clear filter (see Table S3).

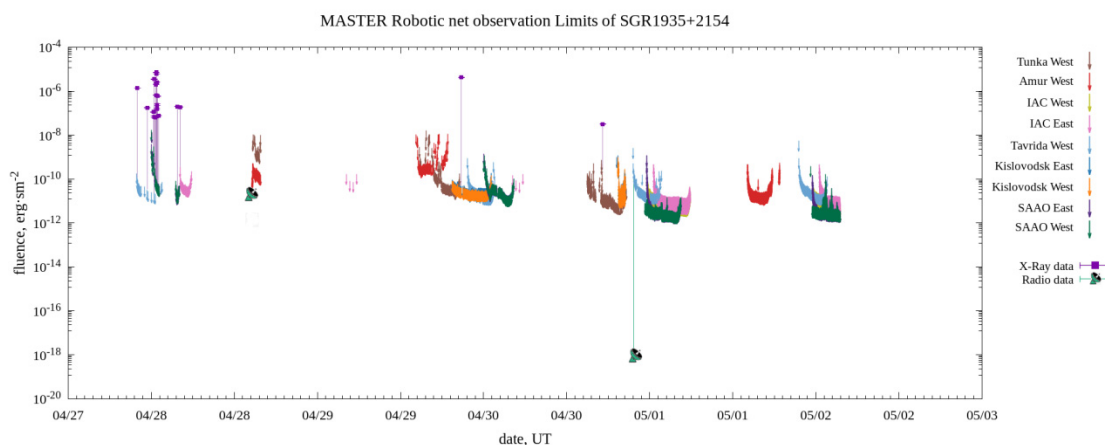


Figure 10. The limiting fluence of optical emission achieved by the MASTER in the process of observing the repeater SGR/FRB 1935+2154. These are not corrected for the Galaxy absorption. The most powerful fluences of the gamma-ray range (Fermi, INSIGHT), which fell at the time of our exposure, are shown in purple. Small radio telescopes show radio fluence on 28 April and 30 April. The second radio burst on April 30 was very weak but was coincident with our frame [90].

Taking this absorption into account, we chose the 20 brightest bursts that coincided with our frames (Table S3). Of these, the 3 best limits for the exponent of the power-law spectrum are shown in Figure 11. Evidently, all three redistributions contradict the power-law spectrum obtained from the data of simultaneous measurements at the time of the radio burst on 28 April. Recall that simultaneous observations of the gamma and radio pulse gave the flux spectrum slope $F \sim \nu^\alpha$, $\alpha \approx 0.46$ [92]. From the observations made by MASTER-Tavrida and Swift, we set a following limit on the slope of a power-law spectrum

$F \sim \nu^\alpha$: $\alpha > 0.57 \pm 0.05$ from 5×10^{14} Hz to 10^{19} Hz. Therefore, at the SNR = 4 level, we reject the observed early tilt of the gamma-radio spectrum.

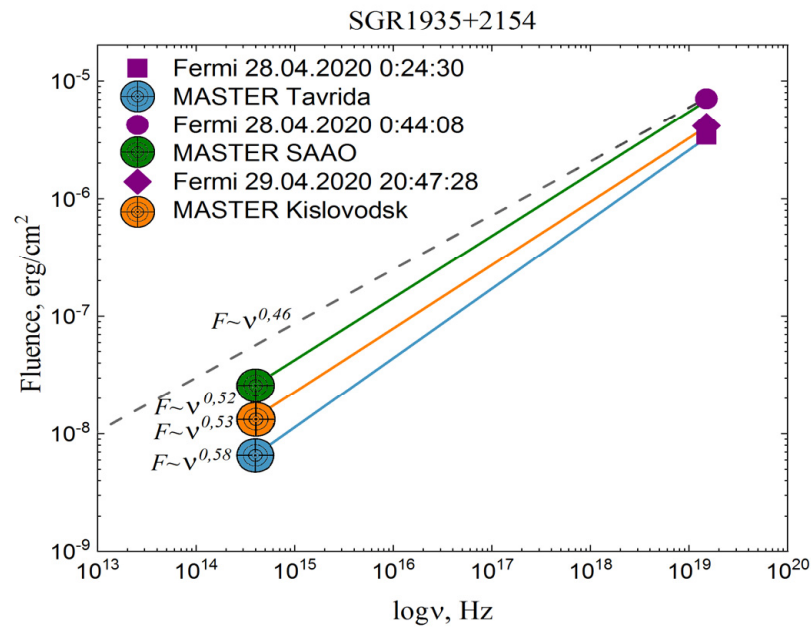


Figure 11. Fluence spectrum of the brightest bursts (Fermi values was taken from [59], MASTER values are our own). Targets show the optical fluence limits obtained by MASTER telescopes, the dashed line corresponds to the power law index deduced from radio and X-ray simultaneous detection.

6. Discussion

A detailed review [93] of possible optical and X-ray radiation from FRBs in different models of magnetar radiation showed that such radiation is quite possible [86] at the level $\eta = \text{Fluence}_{\text{opt}}/\text{Fluence}_{\text{radio}} \sim 10^5$, which in terms of the power-law spectrum corresponds to $\alpha \approx 0.5$.

Currently, two models of magnetar radiation prevail, which make it possible to explain their high brightness temperature, for example, FRBs ($\sim 10^{35}$ K). The first model is laser emission of light-charged particles (leptons) with an inverse energy distribution in a moderately magnetized relativistic shock wave with a large Lorentz factor ($\Gamma \gg 1$, [94]). The second model is that the emission from magnetars, similar to the emission of radio pulsars, arises from the emission caused by the curvature of magnetic field lines [95,96]. However, in contrast to radio pulsar radiation, the acceleration of charged leptons ($\Gamma \sim 30$) is due to reconnection of field lines in the magnetosphere of the magnetar, and not by the polar gap. Some models predicted by Metzger et al. [50] were multi-wavelength counterparts, in the X-ray and gamma range $\eta = \text{Fluence}_x/\text{Fluence}_{\text{radio}} \sim 10^5$.

Fast radio burst detection [89] from soft gamma repeaters directly supports the magnetar model [47–50]. This important discovery means that all the early detected traces of optical radiation from magnetars—soft gamma repeaters or anomalous X-ray pulsars (AXP)—can be considered as real phenomena accompanying FRB sources. However, optical radiation from magnetars has yet to be perceived as short flashes accompanying radio bursts. They have been observed either as flares lasting tens of seconds [97] or as optical pulsations [98]. The optical flux of the pulsating radiation from SGR 0501+4516 in the i' filter was at the level of 24 m. Extrapolating it on galactic distances shows that it is almost impossible to find such radiation from extragalactic FRBs. An interesting topic is the intrinsic radiation of FRB in the optical range to which our study was devoted, and which we will discuss with the help of a diagram (Figure 12) of all known simultaneous observations of FRBs.

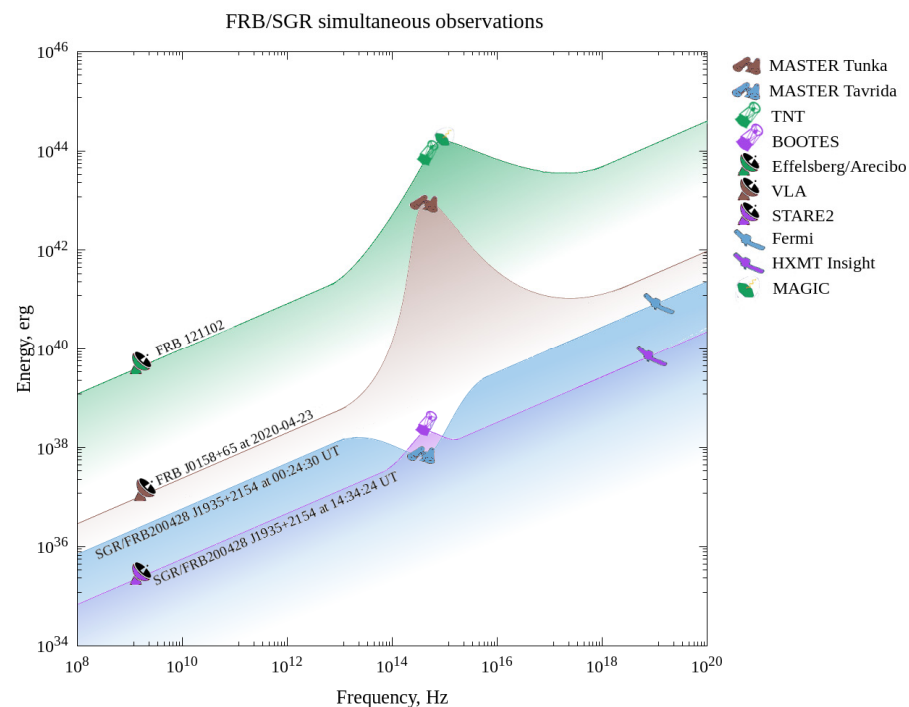


Figure 12. Results of simultaneous observations of fast radio burst sources for 28 April 2020 14:34:24 UT. The first X-ray detection of FRB synchronous with radio emission is shown in purple. Assuming a power-law spectrum, they set the slope on the entire graph $\alpha \approx 0.46$. The X-ray flare of SGR J1935+2154 at 00:24:30 UT on 28 April 2020 and our optical limit from MASTER-Tavrida are shown in blue.

Four synchronous limits in optics are shown in green, brown, blue, and purple. It is clear that only the MASTER limit presented in this article is below the power-law spectrum corresponding to the soft gamma repeater flare. Schematic icons show the optical limits of MASTER (this paper), TNT-Thai National Telescope [99], BOOTES-3 [100], and MAGIC [101]. Radio and X-ray detections are represented by the Effelsberg [99], Arecibo [101], VLA Karl Jansky [77], STARE2 [89], Fermi [59], and Insight-HXMT [10] telescopes.

We present the results of the long monitoring of the FRB. The first synchronous optical observation of the fast radio burster FRB 180916.J0158+65 is presented. Our current limit for FRB 180916.J0158+65 on simultaneous optical fluence is $\eta < 4 \times 10^5$. It does not contradict the predictions of the magnetar model of Chen et al. [93].

This is not the first attempt to investigate the optical properties of the FRB 180916.J0158+65. The most successful observations with a high frame rate were made on the 1.8 m Copernicus telescope using the fast optical photon counter Aqueye+ [102]. However, these observations did not overlap with any radio burst. They set an upper limit for optical radiation outside the radio bursts on $0.012 \text{ Jy} \cdot \text{ms}$, which is close to our sensitivity but much better than the ZTF results ($E_{\text{opt}} < 3 \times 10^{46} \text{ erg}$ for a $10 \text{ Jy} \cdot \text{ms}$ radio burst) due to the significantly shorter exposure time [51]. Kilpatrick et al. [103] observed FRB 180916.J0158+65 contemporaneously with the CHIME only 2 s after the burst but failed to detect any optical transient down to the limiting magnitude of 24.7 in i-band.

Similar studies were conducted with FRB 121102. The 2.4 m Thai National Telescope in collaboration with the 100 m Effelsberg Radio Telescope limited the optical fluence of the FRB 121102 burst: $0.05 \text{ Jy} \cdot \text{ms}$, while radio fluence of the brightest burst was $2.6 \text{ Jy} \cdot \text{ms}$ [99]. Considering the absorption in i-band, these fluences correspond to following energies of the burst: optical— $6 \times 10^{43} \text{ erg}$, radio— $4 \times 10^{39} \text{ erg}$ ($\eta < 1.5 \times 10^4$). MAGIC Collaboration [101] observed FRB 121102 using the basic atmospheric gamma Cherenkov telescope simultaneously with Arecibo. Having observed 5 bursts, they did not find a convincing signal with fluence $> 9 \times 10^{-3} \text{ Jy} \cdot \text{ms}$ at an exposure time of 1 ms. Estimating the fluence

of the burst as peak brightness multiplied by a half of duration, the brightest burst has a fluence of 4 Jy·ms. Considering absorption in U band, these fluences correspond to following energies of the burst: optical 1.6×10^{44} erg, radio 6×10^{39} erg.

However, after the discovery of the simultaneous soft gamma, X-ray, and radio flare SGR/FRB 200428.J1935+2154, we have the observed slope of the spectrum in the approximation of the power law [93] $\alpha \approx 0.46$, and it is shown in Figure 12 by sloped, colored stripes. This makes it possible to visualize the available synchronous multiwavelength observations and understand how they agree with the known slope. Obviously, all available optical observations of FRB 180916.J0158+65, FRB 121102, and SGR/FRB 200428.J1935+2154 lie above the corresponding extrapolation to the optical radiation power and cannot limit the result obtained, though they lie quite close to the estimates of some theoretical models [93].

The first observation of SGR/FRB 200428.J1935+2154 on 28 April 2020 at 14:34:24 UTC in the X-ray, radio, and optical ranges is very important. However, the optical limit turned out to be significantly higher than the power-law extrapolation. Our limits for the source SGR/FRB 200428.J1935+2154, presented here, turned out to be much more significant. The best MASTER limit obtained by us on the MASTER-Tavrida telescope directly shows that the X-ray flares that occurred half a day before the radio flare had a completely different spectrum than the FRB200428, assuming it was still described by a power-law. This excludes a single power-law spectrum for this flare, which is confirmed by the absence of a radio flare at that time [100].

7. MASTER Gravitational Wave LIGO/Virgo Phenomena Investigations

In a compact binary coalescence (CBC) event, a tight binary comprised of two neutron stars (NSs), two black holes (BHs), or an NS and a BH experiences a runaway orbital decay due to gravitational radiation, that since 2015 was registered by aLIGO, LIGO/Virgo collaboration (LVC) [16,17]. MASTER Global Robotic Net observed all LVC events error-fields in O1, O2, O3 epochs. During O1, O2 epoch of observations, gravitational wave events (GW) had very large error-fields [16] (Figure 13). The first one, GW150914, had no zero in initial probability distribution with several maximums, and to observe it effectively, we used our own Central Planner (CP) with the following strategy.

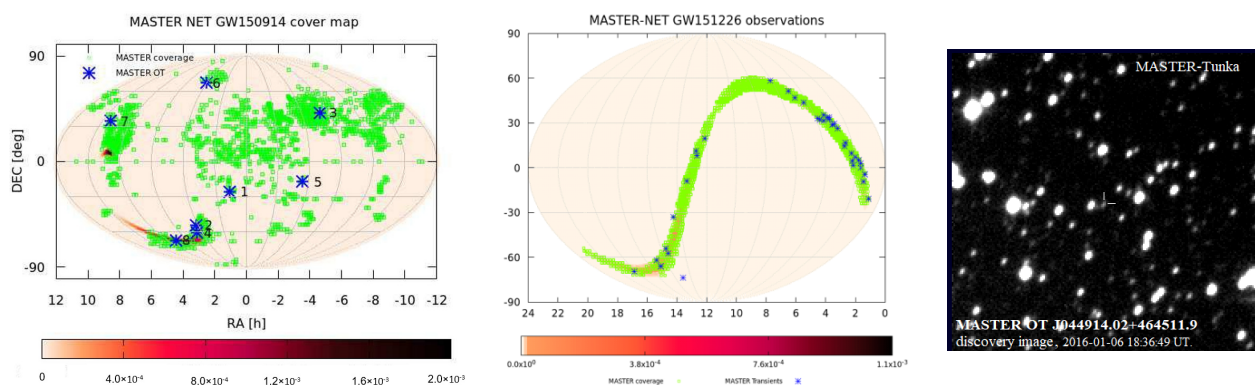


Figure 13. The complete maps of the sky survey carried out by MASTER Net for GW150914 (left) from 14 to 22 September 2015 and for the GW151226 (middle) for 2 weeks, with MASTER OT J044914.02+464511.9 (right) source discovered at the time of inspection at MASTER-Tunka.

So, as MASTER observes GRB error-boxes, HE neutrino error-fields, FRB and GW ones at the same time, the priority of current alert observations depends on (1) the difference between current and trigger/notice time, (2) the size of error-field (Swift, Fermi-LAT, MAXI have bigger priority, then LVC maximum, IceCube, ANTARES, LVC full field, if they all come together). Then, CP automatically distributes targets between MASTER observatories, choosing the current square (2×4 sq.deg., i.e., our FOW) from several criteria, including altitude of maximum probability at current observatory; the availability time for observation, etc. CP operates so as to have the upper limits of each image to be

$m_{\text{lim}} \sim 19\text{--}20$ m as the result of inspection. This strategy let us made a crucial contribution to an optical inspection (>5200 sq.deg.) of GW150914 [16,19], made independently discovered by the Kilonova MASTER OT J130948.10-232253.3 in the NGC 4993 galaxy [17,21] of GW170817 (Figure 14), and to discover a lot of OTs during inspect survey of O1–O3 follow-up optical observations (not connected with BBH merging, but due to the results of MASTER inspect survey, see blue asterisk at Figure 13).



Figure 14. MASTER image of Kilonova (full frame and composed colored).

For example, new optical source MASTER OT J044914.02+464511.9 was discovered by MASTER-Tunka auto-detection system on 6 January 2016 18:36:49 UT (Figure 13) with unfiltered $m_{\text{OT}} = 17.4$ m ($m_{\text{lim}} = 19.7$ m) during GW151226/G211117 (trigger = 26 December 2015 03:38:53) inspection. We covered 4.3% of total probability field synchronously with GW trigger at MASTER-Kislovodsk and MASTER-IAC, and 2915 square degrees in total (82.4% of the 3σ error-box, Figure 13). The OT was seen in 4 images with the same magnitude (18:16:03, 18:36:49, 18:54:27, 19:28:19), so we excluded UV Cet-type of variability. As there are no sources in PanSTARRS ($m_{\text{lim}} = 24$) images and in VIZIER database, we can estimate amplitude of current outburst as >6.6 m (calibrated by red, one value). We have our own reference images (without OT) at 15 April 2015 18:49:11 UT, with an unfiltered $m_{\text{lim}} = 19.0$ m, 2 October 2016 18:49:09 UT with $m_{\text{lim}} = 20.0$, and many others in 2009–2022.

In total, we covered 31,830 sq.deg. in O1 epoch of LVC alerts observation, 62788 sq.deg. in O2 epoch, and 105,380 sq.deg. in O3 one (Table S4).

8. MASTER Investigations of IceCube, ANTARES High Energy Neutrino Phenomena

High energy neutrinos are produced when cosmic rays interact with ambient matter (pp interactions) or photon fields (py interactions). These interactions are expected to happen mainly within cosmic-ray sources where the target photon and/or matter densities are high. The detection of a neutrino source would imply that this source also accelerates cosmic rays. Cosmic rays can be accelerated at collisionless shock fronts which are expected in a wide variety of astrophysical objects. Potential neutrino sources are GRBs, active galactic nuclei, tidal disruption events, and starburst galaxies [35]. Neutrinos can interact and produce secondary particles through neutral current interactions (induced by any neutrino flavor) or through charged current interactions (induced by electron or tau neutrinos), and produce localized, almost spherical light patterns inside the detector, which makes directional reconstructions challenging. Muons produced in ν_μ charge current interactions, can travel up to several kilometers in the ice and emit Cherenkov light along their trajectories. These events (tracks) and their source directions can be reconstructed to better than one degree if their energy is >1 TeV.

MASTER started follow-up observations for IceCube and ANTARES in 2015. On 17 February 2016 19:21:31.65 UTC, several neutrino events, which were later believed to originate from one source, were detected by IceCube(IC) [35]. All three events arrived within less than 100 s and were classified by IC as a triplet and triggered electromagnetic

follow-up campaign (by Swift-XRT, ASAS-SN, LCO, MASTER, and by VERITAS in the very high-energy gamma-ray band), where MASTER contributed the largest optical support (Figure 15a). We received the neutrino triplet coordinates by email at 18 February 2016 17:15:58 UTC, observations started at the MASTER-Kislovodsk within less than one hour, and this position was monitored by MASTER-Tunka and MASTER-IAC for the following month [35].

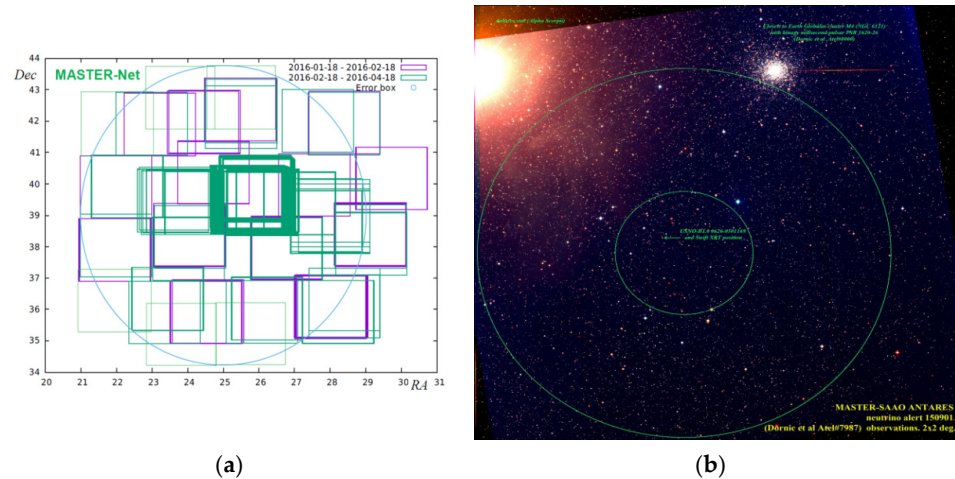


Figure 15. (a) MASTER cover map of IceCube IC160217 triplet error-box, observed by -Kislovodsk, -Tunka, -IAC telescopes during 1 month before trigger (magenta squares 18 January / February 2016) and 2 months after (green); (b) MASTER image of ANTARES alert ANT 150901.32 [36] M5 globular cluster, Swift transient (the source was stable in optic in BVRI), and Antares star (1.3 deg. from the 3- σ error-box center) are marked.

On 1 September 2015 07:38:24, ANTARES neutrino observatory registered a neutrino event (R.A., Dec(J2000) = 16:25:42, +27:23:24; $r = 1.7$ deg) and MASTER started alert observations in -SAAO ($t_{\text{start}} = 17:13:59$ UT, $m_{v,\text{lim}} = 19.9$), -IAC ($t_{\text{start}} = 21:02:44$, $m_{B,\text{lim}} = 19.8$), -Kislovodsk (3 September 2015 17:21:39 UT, unfiltered $m_{\text{lim}} = 18.9$) and -Tunka (3 September 2015 12:40:59 UT) (Figure 15b). There is Globular Cluster M4 (NGC621) with a millisecond pulsar and a possible massive black hole inside 3-sigma error-box, proposing M4 with relativistic objects inside as the possible source of the neutrino, which was created after cosmic particle acceleration.

Of the 179 ANTARES neutrino alerts received by the MASTER, which surveyed their arrival areas, only 20 high energy neutrino events contain blazars in the error-box arrival with a radius of no more than 0.7 deg. The optical variability of blazars 5BZBJ2256-3303 from ANT181108A neutrino event error-box and PMN_J2345-1555 from ANT160111A are presented in Figure 16.

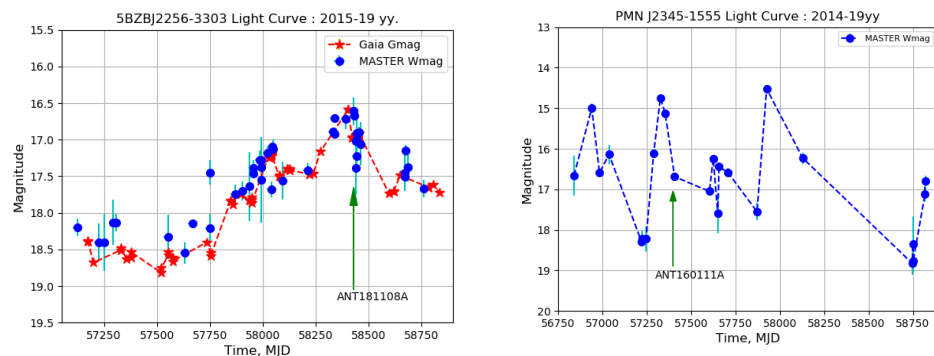


Figure 16. Optical variability of the blazars 5BZBJ2256-3303 and PMN_J2345-1555 according to the MASTER data (and Gaia for left one). The arrow indicates HE ANTARES neutrino event ANT181108A (left) and ANT160111A (right).

In 2017, between GW and GRB alerts, we received (by GCN) IceCube-170922A alert (trigger time 22 September 2017 20:54:30 UT). MASTER-Tavrida automatically carried out the earliest astronomical observation of this error-box, 27 s after notice time (73 s after trigger time, $T_{\text{start}} = 22 \text{ September } 2017 \text{ } 20:55:43$), of which the blazar TXS 0506+056 variability was discovered just after high energy neutrino detection. The earliest astronomical observation of IC-170922A, conducted by us, ref. [25] allowed us to find the blazar TXS 0506+056 in a dim state several minutes after the neutrino detection and to then return to its previous bright state two hours after the event. We observed this effect at a 50σ significance level. Our 16y light curve archive and light curve of blazar TXS 0506+056 (518 data set during 2005–2020yy) is presented in Figure 17. We represent three very narrow episodes in time in this figure. The first one was in 2015 April when IceCube IC86b saw a 3.5σ excess of the neutrino flux over the background. The second one was in 2017. Just our observations demonstrate the decrease of the brightness of the TXS 0506+056 blazar near the neutrino detection time, and provides complementary and very compelling evidence for the link between the blazar and the IceCube-170922 neutrino event [25]. We find that, for the adopted set of cosmological parameters $H_0 = 67.8 \text{ km}/(\text{s Mpc})$, the matter and vacuum density $\Omega_m = 0.308$, and $\Omega_\Lambda = 0.692$, a few minutes after the neutrino trigger, optical isotropic luminosity of the blazar was $L_{\text{opt}} \sim 4.3 \times 10^{45} \text{ erg/s}$ and after two hours, it returned to the typical level within several weeks of the neutrino event, $\sim 9.7 \times 10^{45} \text{ erg/s}$. We noticed that optical radiation can also be produced as synchrotron radiation of protons in a zone with a reduced magnetic field. Then, it should be expected that with an increase in the neutrino flux, due to the disappearance of protons in pp-reactions, the optical synchrotron photons of the p will drop. The maximal amplitude of the decrease in optical luminosity can be as much as 2 times, since the branches of the reaction proceed with approximately the same probability, as we observed.

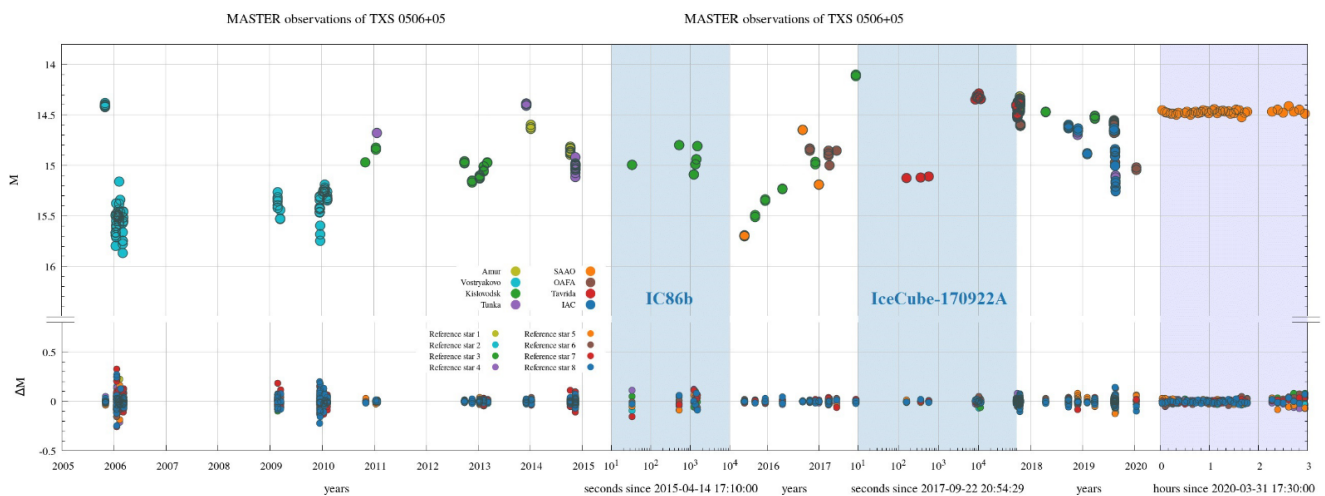


Figure 17. MASTER light curve of the TXS 0506+056 blazar for 16 y. Below, we see the photometry of eight reference stars. The pink and blue panels represent three very narrow episodes in time. One can see the rapid change in the luminosity of the blazar in ~ 2 times. Finally, the third episode is a uniform blazar monitoring timeline in the first quarter of 2020. Logarithmic time is shown in seconds from the neutrino trigger in pink panel [25] ©MASTER2020.

9. Conclusions

We presented MASTER Global Robotic Net real-time multi-message observations of high energy phenomena results, including investigations in gamma-ray astronomy, gravitational wave astronomy, high energy neutrino astronomy, and FRB.

In FRB investigations, our optical observations may mean that optical, radio, and soft gamma radiation are not described by a universal power-law spectrum and can occur in different regions of the magnetosphere of a neutron star—a magnetar. This is quite consistent with the findings of the Konus-Wind team [13]. Moreover, it is quite natural

that particles of different energies in different parts of the magnetosphere can be emitted sequentially or independently, which was observed during a radio flare on 28 April 2020.

Recently, Hubble data (Hubble Space Telescope observations) has demonstrated that FRB 20180916B is slightly offset from the nearby star-forming regions, 0.37 arcseconds to be exact [104]. However, our image is much rougher: $\text{FWHM} = 2.5 \times 2'' = 5''$ and we cannot separate the contribution from the star-forming zone. Therefore, we cannot improve our limit on its optical emission.

We would not like to narrow FRB down to one type of source, discarding, perhaps, genetically related, but physically different phenomena. For example, the merger of neutron stars is currently considered as a probable channel for the formation of magnetars [105–110]. If this is confirmed, then a unique fusion event may become the site of sporadic or periodic outbreaks after a while.

Supplementary Materials: The following supporting information can be downloaded at: <https://www.mdpi.com/article/10.3390/universe8050271/s1>, Table S1: Objects detected simultaneously in two MASTER-Kislovodsk east and west cameras in place of the FRB, and in two randomly selected empty places. A group of 3 pixels, each of which exceeds the background level by 1 sigma was called an object; Table S2: The photometry of the galactic star formation region from Gemini fit around FRB 180916.J0158+65; Table S3: Bright events SGR/FRB 200428.J1935+2154 simultaneously observed by MASTER Global Network telescopes in April 2020 of the, we compared them with Fermi/GBM [100], HXMT Insight [10], FAST [90]; Table S4: Results of aLIGO, LIGO/Virgo O1, O2, O3 alerts and optical observations coverage at MASTER-Amur, -Tunka (Tun), -Kislovodsk(Kis), -Tavrida (Tav), -IAC, -SAAO(SA), -OFA robotic telescopes.

Author Contributions: Idea of all experiment, algorithm, observations: V.M.L. and V.G.K., data curation: V.M.L., V.G.K., K.Z., A.K., E.G., N.M.B., D.A.H.B., R.R.L., M.S.-R., C.F., N.T., O.G., P.B., G.A., D.V., V.T., A.C., S.I.S., R.P., F.P., E.M., A.G.T., V.V.Y., A.G., O.E., V.S. and D.K. All authors have read and agreed to the published version of the manuscript.

Funding: N.G.B. is supported by the RFMSH (FZZE-2020-0017). E.G. is supported by the Rfbr 19-29-11011. A.C. is supported by BAZIS21-2-1-135-1.

Acknowledgments: First of all, we would like to express our deep gratitude to Scott Barthelmy for the creation and long-term support of the Gamma Center Network (<https://gcn.gsfc.nasa.gov> accessed on 1 March 2022), which is the key factor in the field of multi-messenger astronomy, including our research. The authors are grateful to Yu. E. Lyubarsky for a useful discussion of the results reported in this paper. We acknowledge support by the Development Program of Lomonosov Moscow State University (MASTER equipment). The research is carried out using the equipment of the shared research facilities of HPC computing resources at Lomonosov Moscow State University [111]. DAHB acknowledges support through the National Research Foundation (NRF) of South Africa. MASTER- Tunka work was performed using the UNU «Astrophysical Complex of MSU-ISU» facility (agreement 13.UNU.21.0007). The image of the galaxy [52], <http://master.sai.msu.ru/images/universe/figure7a.jpg> (accessed on 1 March 2022), was taken from public Gemini archive https://archive.gemini.edu/searchform/not_site_monitoring/GMOS-N/NotFail/cols=CTOWEQ/GN-2019A-DD-10/notengineering (accessed on 1 March 2022) and MASTER data.

Conflicts of Interest: The authors declare no conflict of interest.

References

1. Chatterjee, S.; Law, C.; Wharton, R.S.; Burke-Spolaor, S.; Hessels, J.W.T.; Bower, G.; Cordes, J.M.; Tendulkar, S.P.; Bassa, C.G.; Demorest, P.; et al. A direct localization of a fast radio burst & its host. *Nature* **2017**, *541*, 58–61. [PubMed]
2. CHIME/FRB Collaboration. A second source of repeating fast radio bursts. *Nature* **2019**, *566*, 235–238. [CrossRef] [PubMed]
3. The CHIME/FRB Collaboration. CHIME/FRB Detection of Eight New Repeating Fast Radio Burst Sources. *Astrophys. J. Lett.* **2019**, *885*, L24. [CrossRef]
4. The CHIME/FRB Collaboration. A bright millisecond-duration radio burst from a Galactic magnetar. *Nature* **2020**, *587*, 54–58. [CrossRef]
5. Lipunov, V.; Kornilov, V.; Gorbovskoy, E.; Shatskij, N.; Kuvshinov, D.; Tyurina, N.; Belinski, A.; Krylov, A.; Balanutsa, P.; Chazov, V.; et al. MASTER Robotic Net. *Advan. Astron.* **2010**, *2010*, 349171. [CrossRef]

6. Lipunov, V.M.; Vladimirov, V.V.; Gorbovskoi, E.S.; Kuznetsov, A.S.; Zimnukhov, D.S.; Balanutsa, P.V.; Kornilov, V.G.; Tyurina, N.V.; Gress, O.A.; Vlasenko, D.M.; et al. The Concept of a Multi-Functional Astronomy Complex & Dynamically Integrated Database Applied to Multi-Channel Observations with the MASTER Global Network. *Astron. Rep.* **2019**, *63*, 293–309.
7. Kornilov, V.G.; Lipunov, V.M.; Gorbovskoy, E.S.; Belinski, A.; Kuvshinov, D.A.; Tyurina, N.V.; Shatsky, N.I.; Sankovich, A.V.; Krylov, A.V.; Balanutsa, P.V.; et al. Robotic optical telescopes global network MASTER II. Equipment, structure, algorithms. *Exp. Astron.* **2012**, *33*, 173–196. [[CrossRef](#)]
8. Sadovnichy, V.A.; Panasyuk, M.I.; Svertilov, S.I.; Lipunov, V.M.; Bogomolov, V.V.; Gorbovskoy, E.S.; Castro-Tirado, A.J.; Gabovich, A.; Hu, Y.; Iyudin, A.F.; et al. Prompt & Follow-up Multi-wavelength Observations of the GRB 161017A. *Astrophys. J.* **2018**, *861*, 48.
9. Li, C.K.; Lin, L.; Xiong, S.L.; Ge, M.Y.; Li, X.B.; Li, T.P.; Lu, F.J.; Zhang, S.N.; Tuo, Y.L.; Nang, Y.; et al. Identification of a non-thermal X-ray burst with the Galactic magnetar SGR 1935+2154 & a fast radio burst with Insight-HXMT. *Nat. Astron.* **2021**, *5*, 378–384.
10. Li, C.; Cai, C.; Zhang, S.-N.; Xiong, S.-L.; Li, X.-B.; Ge, M.-Y.; Jia, S.-M.; Nie, J.-Y.; Zhao, H.-S.; Liu, C.-Z.; et al. Updated catalog of X-ray bursts of SGR J1935+2154 from Insight-HXMT observations. *GCN Circ.* **2020**, 28027, 1.
11. Mereghetti, S.; Savchenko, V.; Ferrigno, C.; Götz, D.; Rigoselli, M.; Tiengo, A.; Bazzano, A.; Bozzo, E.; Coleiro, A.; Courvoisier, T.J.-L.; et al. INTEGRAL discovery of a burst with associated radio emission from the magnetar SGR 1935+2154. *Astrophys. J. Lett.* **2020**, *898*, L29. [[CrossRef](#)]
12. Tavani, M.; Casentini, C.; Ursi, A.; Verrecchia, F.; Addis, A.; Antonelli, L.A.; Argan, A.; Barbiellini, G.; Baroncelli, L.; Bernardi, G.; et al. An X-ray burst from a magnetar enlightening the mechanism of fast radio bursts. *Nat. Astron.* **2021**, *5*, 401–407. [[CrossRef](#)]
13. Ridnaia, A.; Svinkin, D.; Frederiks, D.; Bykov, A.; Popov, S.; Aptekar, R.; Golenetskii, S.; Lysenko, A.; Tsvetkova, A.; Ulanov, M.; et al. A peculiar hard X-ray counterpart of a Galactic fast radio burst. *Nat. Astron.* **2021**, *5*, 372–377. [[CrossRef](#)]
14. Klebesadel, R.W.; Strong, I.B.; Olson, R.A. Observations of Gamma-ray Bursts of Cosmic Origin. *Astrophys. J.* **1973**, *182*, L85–L89. [[CrossRef](#)]
15. Mazets, E.P.; Golenetsky, S.V.; Ilinskiy, V.N. Burst of cosmic gamma-emission from observations on Cosmos 461. *PZETF* **1974**, *19*, 126–128.
16. Abbott, B.P.; Abbott, R.; Abbott, T.D.; Abernathy, M.R.; Acernese, F.; Ackley, K.; Adams, C.; Adams, T.; Addesso, P.; Adhikari, R.X.; et al. Localization and Broadband Follow-up of the Gravitational-wave Transient GW150914. *Astrophys. J. Lett.* **2016**, *826*, L13. [[CrossRef](#)]
17. Abbott, B.P.; Abbott, R.; Abbott, T.D.; Acernese, F.; Ackley, K.; Adams, C.; Adams, T.; Addesso, P.; Adhikari, R.X.; Adya, V.B.; et al. Multi-messenger Observations of a Binary Neutron Star Merger. *Astrophys. J. Lett.* **2017**, *848*, L12.
18. Lipunov, V.M. Astrophysical meaning of the discovery of gravitational waves. *Phys.-Uspekhi* **2016**, *59*, 918. [[CrossRef](#)]
19. Lipunov, V.M.; Kornilov, V.; Gorbovskoy, E.; Buckley, D.A.H.; Tiurina, N.; Balanutsa, P.; Kuznetsov, A.; Greiner, J.; Vladimirov, V.; Vlasenko, D.; et al. First gravitational-wave burst GW150914: MASTER optical follow-up observations. *Mon. Not. R. Astron. Soc.* **2017**, *465*, 3656–3667. [[CrossRef](#)]
20. Lipunov, V.M.; Kornilov, V.; Gorbovskoy, E.; Tiurina, N.; Balanutsa, P.; Kuznetsov, A. The first gravitational-wave burst GW150914, as predicted by the scenario machine. *New Astron.* **2017**, *51*, 122–127. [[CrossRef](#)]
21. Lipunov, V.M.; Gorbovskoy, E.; Kornilov, V.G.; Tyurina, N.; Balanutsa, P.; Kuznetsov, A.; Vlasenko, D.; Kuvshinov, D.; Gorbunov, I.; Buckley, D.A.H.; et al. MASTER Optical Detection of the First LIGO/Virgo Neutron Star Binary Merger GW170817. *Astrophys. J. Lett.* **2017**, *850*, L1. [[CrossRef](#)]
22. Lipunov, V.M.; Postnov, K.A.; Prokhorov, M.E. First LIGO events: Binary black holes merging. *New Astron.* **1997**, *2*, 43–52. [[CrossRef](#)]
23. Lipunov, V.M.; Postnov, K.A.; Prokhorov, M.E. Formation and coalescence of relativistic binary stars: The effect of kick velocity. *Mon. Not. R. Astron. Soc.* **1997**, *288*, 245–259. [[CrossRef](#)]
24. Lipunov, V.M.; Postnov, K.A.; Prokhorov, M.E. Black holes and gravitational waves: Possibilities for simultaneous detection using first-generation laser interferometers. *Astron. Lett.* **1997**, *23*, 492–497.
25. Lipunov, V.M.; Kornilov, V.G.; Zhirkov, K.; Gorbovskoy, E.; Budnev, N.M.; Buckley, D.A.H.; Rebolo, R.; Serra-Ricart, M.; Podesta, R.; Tyurina, N.; et al. Optical Observations Reveal Strong Evidence for High-energy Neutrino Progenitor. *Astrophys. J. Lett.* **2020**, *896*, L19. [[CrossRef](#)]
26. Abbott, B.P.; Abbott, R.; Abbott, T.D.; Acernese, F.; Ackley, K.; Adams, C.; Adams, T.; Addesso, P.; Adhikari, R.X.; Adya, V.B.; et al. A gravitational-wave standard siren measurement of the Hubble constant. *Nature* **2017**, *551*, 85.
27. Troja, E.; Lipunov, V.M.; Mundell, C.G.; Butler, N.R.; Watson, A.M.; Kobayashi, S.; Cenko, S.B.; Marshall, F.E.; Ricci, R.; Fruchter, A.; et al. Significant & variable linear polarization during the prompt optical flash of GRB 160625B. *Nature* **2017**, *547*, 425–427.
28. Lipunov, V.; Simakov, S.; Gorbovskoy, E.; Vlasenko, D. Smooth Optical Self-similar Emission of Gamma-ray Bursts. *Astrophys. J.* **2017**, *845*, 52. [[CrossRef](#)]
29. Lipunov, V.; Kornilov, V.; Gorbovskoy, E.; Tiurina, N.; Kuznetsov, A.; Balanutsa, P.; Chazov, V.; Gress, O.; Kuvshinov, D.; Vladimirov, V.; et al. MASTER Global Robotic Net: New sites and new results. *Rev. Mex. AC* **2016**, *48*, 42L.

30. Lipunov, V.M.; Gorosabel, J.; Pruzhinskaya, M.V.; Postigo, A.d.; Pelassa, V.; Tsvetkova, A.E.; Sokolov, I.V.; Kann, D.A.; Xu, D.; Gorbvskoy, E.S.; et al. The optical identification of events with poorly defined locations: The case of the Fermi GBM GRB 140801A. *Mon. Not. Roy. Astron. Soc.* **2016**, *45*, 712. [\[CrossRef\]](#)
31. Jordana-Mitjans, N.; Mundell, C.G.; Kobayashi, S.; Smith, R.J.; Guidorzi, C.; Steele, I.A.; Shrestha, M.; Gomboc, A.; Marongiu, M.; Martone, R.; et al. Lowly Polarized Light from a Highly Magnetized Jet of GRB 190114C. *Astrophys. J.* **2020**, *892*, 97. [\[CrossRef\]](#)
32. Gorbvskoy, E.S.; Lipunov, V.M.; Buckley, D.A.H.; Kornilov, V.G.; Balanutsa, P.V.; Tyurina, N.V.; Kuznetsov, A.S.; Kuvshinov, D.A.; Gorbunov, I.A.; Vlasenko, D.; et al. Early polarization observations of the optical emission of gamma-ray bursts: GRB 150301B and GRB 150413A. *Mon. Not. R. Astron. Soc.* **2016**, *455*, 3312–3318. [\[CrossRef\]](#)
33. Laskar, T.; van Eerten, H.; Schady, P.; Mundell, C.G.; Alexander, K.D.; Duran, R.B.; Berger, E.; Bolmer, J.; Chornock, R.; Coppejans, D.L.; et al. A Reverse Shock in GRB 181201A. *Astrophys. J.* **2019**, *884*, 121. [\[CrossRef\]](#)
34. Ershova, O.; Lipunov, V.M.; Gorbvskoy, E.S.; Tyurina, N.V.; Kornilov, V.G.; Zimmukhov, D.S.; Gabovich, A.; Gress, O.A.; Budnev, N.M.; Yurkov, V.V.; et al. Early Optical Observations of Gamma-ray Bursts Compared with Their Gamma- & X-ray Characteristics Using a MASTER Global Network of Robotic Telescopes from Lomonosov Moscow State University. *Astron. Rep.* **2020**, *64*, 126–158.
35. Aartsen, M.G.; Ackermann, M.; Adams, J.; Aguilar, J.A.; Ahlers, M.; Ahrens, M.; Al Samarai, I.; Altmann, D.; Andeen, K.; Anderson, T.; et al. Multiwavelength follow-up of a rare IceCube neutrino multiplet. *Astron. Astrophys.* **2017**, *607*, A115.
36. Gress, O.A.; Lipunov, V.M.; Dornic, D.; Gorbvskoy, E.; Kornilov, V.G.; Tyurina, N.V.; Balanutsa, P.V.; Kuznetsov, A.S.; Vladimirov, V.V.; Kuvshinov, D.A. MASTER Investigation of ANTARES and IceCube Alerts. *Rev. Mex. Astron. Astrofisica Ser. Conf.* **2019**, *51*, 89–95. [\[CrossRef\]](#)
37. Lipunov, V.M.; Blinnikov, S.; Gorbvskoy, E.; Tutukov, A.; Baklanov, P.; Krushinski, V.; Tiurina, N.; Balanutsa, P.; Kuznetsov, A.; Kornilov, V.; et al. MASTER OT J004207.99+405501.1/M31LRN 2015 luminous red nova in M31: Discovery, light curve, hydrodynamics and evolution. *Mon. Not. R. Astron. Soc.* **2017**, *470*, 2339. [\[CrossRef\]](#)
38. Lipunov, V.; Gorbvskoy, E.; Afanasiev, V.; Tatarnikova, A.; Denisenko, D.; Makarov, D.; Tiurina, N.; Krushinsky, V.; Vinokurov, A.; Balanutsa, P.; et al. Discovery of an unusual bright eclipsing binary with the longest known period: TYC 2505-672-1/MASTER OT J095310.04+335352.8. *Astron. Astrophys.* **2016**, *588*, A90. [\[CrossRef\]](#)
39. Zimmukhov, D.S.; Lipunov, V.M.; Gorbvskoy, E.S.; Kornilov, V.G.; Tyurina, N.V.; Chazov, V.V.; Gabovich, A.V.; Balanutsa, P.V.; Vladimirov, V.V.; Gress, O.A.; et al. The MASTER Global Robotic Telescope Network: Observations of Asteroid NEA 2015 TB145. *Astron. Rep.* **2019**, *63*, 1056–1068. [\[CrossRef\]](#)
40. Lipunov, V.M.; Gorbvskoy, E.S.; Kornilov, V.G.; Chazov, V.V.; Panasyuk, M.I.; Svertilov, S.I.; Yashin, I.V.; Petrov, V.L.; Kallegae, V.V.; Amelushkin, A.A.; et al. Observations of Near-Earth Optical Transients with the Lomonosov Space Observatory. *Astron. Rep.* **2017**, *62*, 426. [\[CrossRef\]](#)
41. Lipunov, V.M.; Gorbvskoy, E.S.; Kornilov, V.G.; Panasyuk, M.I.; Amelushkin, A.M.; Petrov, V.L.; Yashin, I.V.; Svertilov, S.I.; Vedenkin, N.N. SHOK—The First Russian Wide-Field Optical Camera in Space. *Space Sci. Rev.* **2018**, *214*, 6. [\[CrossRef\]](#)
42. Lorimer, D.R.; Bailes, M.; McLaughlin, M.A.; Narkevic, D.J.; Crawford, F. A Bright Millisecond Radio Burst of Extragalactic Origin. *Science* **2007**, *318*, 777–780. [\[CrossRef\]](#) [\[PubMed\]](#)
43. Petroff, E.; Hessels, J.W.T.; Lorimer, D.R. Fast radio bursts. *Astron. Astrophys. Rev.* **2019**, *27*, 4–79. [\[CrossRef\]](#)
44. Lipunov, V.M.; Panchenko, E. Pulsars revived by gravitational waves. *Astron. Astrophys.* **1996**, *312*, 937–940.
45. Lipunov, V.M.; Pruzhinskaya, M.V. Scenario Machine: Fast radio bursts, short gamma-ray burst, dark energy & Laser Interferometer Gravitational-wave Observatory silence. *Mon. Not. R. Astron. Soc.* **2014**, *440*, 1193–1199.
46. Abbott, R.; Abbott, T.D.; Abraham, S.; Acernese, F.; Ackley, K.; Adams, A.; Adams, C.; Adhikari, R.X.; Adya, V.B.; Affeldt, C.; et al. GWTC-2: Compact Binary Coalescences Observed by LIGO and Virgo during the First Half of the Third Observing Run. *Phys. Rev. X* **2021**, *11*, 021053. [\[CrossRef\]](#)
47. Popov, S.B.; Postnov, K.A. Millisecond extragalactic radio bursts as magnetar flares. *arXiv* **2013**, arXiv:1307.4924.
48. Lyubarsky, Y. A model for fast extragalactic radio bursts. *Mon. Not. R. Astron. Soc.* **2014**, *442*, L9–L13. [\[CrossRef\]](#)
49. Beloborodov, A.M. A Flaring Magnetar in FRB 121102. *Astrophys. J. Lett.* **2017**, *843*, L26. [\[CrossRef\]](#)
50. Metzger, B.D.; Margalit, B.; Sironi, L. Fast radio bursts as synchrotron maser emission from decelerating relativistic blast waves. *Mon. Not. R. Astron. Soc.* **2019**, *485*, 4091–4106. [\[CrossRef\]](#)
51. Andreoni, I.; Lu, W.B.; Smith, R.M.; Masci, F.J.; Bellm, E.C.; Graham, M.J.; Kaplan, D.L.; Kasliwal, M.M.; Kaye, S.; Kupfer, T.; et al. Zwicky Transient Facility constraints on the optical emission from the nearby repeating FRB 180916.J0158+65. *Astrophys. J. Lett.* **2020**, *896*, L2. [\[CrossRef\]](#)
52. Marcote, B.; Nimmo, K.; Hessels, J.W.T.; Tendulkar, S.P.; Bassa, C.G.; Paragi, Z.; Keimpema, A.; Bhardwaj, M.; Karuppusamy, R.; Kaspi, V.M.; et al. A repeating fast radio burst source localized to a nearby spiral galaxy. *Nature* **2020**, *577*, 190. [\[CrossRef\]](#) [\[PubMed\]](#)
53. Amiri, M.; Andersen, B.C.; Bandura, K.M.; Bhardwaj, M.; Boyle, P.J.; Brar, C.; Chawla, P.; Chen, T.; Cliche, J.F.; Cubranic, D.; et al. Periodic activity from a fast radio burst source. *Nature* **2020**, *582*, 351–355.
54. Lien, A.Y.; Barthelmy, S.D.; Baumgartner, W.H.; Cummings, J.R.; Gehrels, N.; Krimm, H.A.; Markwardt, C.B.; Palmer, D.M.; Sakamoto, T.; Stamatikos, M.; et al. GRB 140705A: Swift-BAT refined analysis of a possible newly discovered SGR 1935+2154. *GCN Circ.* **2014**, 16522, 1.

55. Sun, X.H.; Reich, M.; Han, J.L.; Wielebinski, R.; Wang, W.; Müller, P. A Sino-German $\lambda 6$ cm polarization survey of the Galactic plane. *Astron. Astrophys.* **2020**, *536*, A83. [\[CrossRef\]](#)
56. Kozlova, A.V.; Israel, G.L.; Svinkin, D.S.; Frederiks, D.D.; Pal'shin, V.D.; Tsvetkova, A.E.; Hurley, K.; Goldsten, J.; Golovin, D.V.; Mitrofanov, I.G.; et al. The first observation of an intermediate flare from SGR 1935+2154. *Mon. Not. R. Astron. Soc.* **2016**, *460*, 2008–2014. [\[CrossRef\]](#)
57. Zhou, P.; Zhou, X.; Chen, Y.; Wang, J.-S.; Vink, J.; Wang, Y. Revisiting the distance, environment and supernova properties of SNR G57.2+0.8 that hosts SGR 1935+2154. *Astrophys. J.* **2020**, *905*, 99. [\[CrossRef\]](#)
58. Zhong, S.Q.; Dai, Z.G.; Zhang, H.M.; Deng, C.M. On the Distance of SGR 1935+2154 Associated with FRB 200428 and Hosted in SNR G57.2+0.8. *Astrophys. J.* **2020**, *898*, L5. [\[CrossRef\]](#)
59. Lin, L.; Göğüş, E.; Roberts, O.J.; Kouveliotou, C.; Kaneko, Y.; van der Horst, A.J.; Younes, G. Burst Properties of the Most Recurring Transient Magnetar SGR J1935+2154. *Astrophys. J.* **2020**, *893*, 156. [\[CrossRef\]](#)
60. Israel, G.L.; Esposito, P.; Rea, N.; Coti Zelati, F.; Tiengo, A.; Campana, S.; Mereghetti, S.; Rodriguez Castillo, G.A.; Götz, D.; Burgay, M.; et al. The discovery, monitoring and environment of SGR J1935+2154. *Mon. Not. R. Astron. Soc.* **2016**, *457*, 3448–3456. [\[CrossRef\]](#)
61. Barthelmy, S.; Bernardini, M.G.; D'Avanzo, P.; Gropp, J.D.; Kennea, J.A.; Lien, A.Y.; Melandri, A.; Palmer, D.M.; Sbarrato, T.; Siegel, M.H. Swift detection of multiple bursts from SGR 1935+2154. *GCN Circ.* **2020**, 27657, 1.
62. Palmer, D.M. A Forest of Bursts from SGR 1935+2154. *GCN Circ.* **2020**, 27665, 1.
63. Younes, G.; Guver, T.; Enoto, T.; Arzoumanian, A.; Gendreau, K.; Hu, C.P.; Ray, P.S.; Kouveliotou, C.; Guillot, S.; Ho, W.C.G.; et al. Burst forest from SGR 1935+2154 as detected with NICER. *Astron. Telegr.* **2020**, 13678, 1.
64. Gorbovskey, E.S.; Lipunov, V.M.; Kornilov, V.G.; Belinski, A.A.; Kuvshinov, D.A.; Tyurina, N.V.; Sankovich, A.V.; Krylov, A.V.; Shatskiy, N.I.; Balanutsa, P.V.; et al. The MASTER-II network of robotic optical telescopes: First results. *Astron. Rep.* **2013**, *57*, 233. [\[CrossRef\]](#)
65. Tyurina, N.; Lipunov, V.; Kornilov, V.; Gorbovskey, E.; Shatskiy, N.; Kuvshinov, D.; Balanutsa, P.; Belinski, A.; Krushinsky, V.; Zalozhnyh, I.; et al. MASTER Prompt and Follow-Up GRB Observations. *Adv. Astron.* **2010**, *2010*, 763629. [\[CrossRef\]](#)
66. Lipunov, V.; Balakin, F.; Gorbovskey, E.; Kornilov, V.; Tyurina, N.; Balanutsa, P.; Kuznetsov, A.; Balakin, F.; Vladimirov, V.; Vlasenko, D.; et al. FRB 190806: MASTER optical observation. *GCN Circ.* **2019**, 25314, 1.
67. Lipunov, V.; Tyurina, N.; Gorbovskey, E.; Kornilov, V.; Kuznetsov, A.; Chazov, V.; Gorbunov, I.; Zimnukhov, D.; Kuvshinov, D.; Balanutsa, P.; et al. FRB 180725A: MASTER optical observations of the Fast Radio Burst error box. *GCN Circ.* **2018**, 23070, 1.
68. Lipunov, V.; Gorbovskey, E.; Rebolo, R.; Serra-Ricart, M.; Balanutsa, P.; Tyurina, N.; Kornilov, V.; Vlasenko, D.; Gress, O.; Budnev, N.; et al. MASTER Net: FRB 180725A observations. *Astron. Telegr.* **2018**, 11902, 1.
69. Balanutsa, P.; Lipunov, V. MASTER follow up inspection of the FRB 180714 error box. *Astron. Telegr.* **2018**, 11880, 1.
70. Balakin, F.; Lipunov, V.; Gorbovskey, E.; Kornilov, V.; Tyurina, N.; Balanutsa, P.; Kuznetsov, A.; Balakin, F.; Vladimirov, V.; Vlasenko, D.; et al. MASTER follow-up of FRB 190806. *Astron. Telegr.* **2019**, 13017, 1.
71. Lipunov, V.; Minkina, E.; Kornilov, V.; Gorbovskey, E.; Tyurina, N.; Zhirkov, K.; Gress, O.; Balanutsa, P.; Gorbunov, I.; Kuznetsov, A.; et al. MASTER optical observations of UTMOST FRB 200607. *Astron. Telegr.* **2020**, 13793, 1.
72. Balakin, F.; Lipunov, V.; Gorbovskey, E.; Tyurina, N.; Kornilov, V.; Vlasenko, D.; Vladimirov, V.; Zimnukhov, D.; Kuznetsov, A.; Balanutsa, P.; et al. FRB190322: MASTER optical observations. *Astron. Telegr.* **2019**, 12612, 1.
73. Gorbovskey, E.; Balakin, F.; Lipunov, V.; Kornilov, V.; Tyurina, N.; Balanutsa, P.; Kuznetsov, A.; Vlasenko, D.; Vladimirov, V.; Zimnukhov, D.; et al. MASTER PSN Discovery During FRB181228 Error Line Inspection. *Astron. Telegr.* **2018**, 12338, 1.
74. Gorbovskey, E.; Lipunov, V.; Tyurina, N.; Kornilov, V.; Balanutsa, P.; Kuznetsov, A.; Vlasenko, D.; Balakin, F.; Podesta, R.; Lopez, C.; et al. FRB 181228: Global MASTER Net optical inspection. *GCN Circ.* **2018**, 23587, 1.
75. Lipunov, V.; Gorbovskey, E.; Tyurina, N.; Kornilov, V.; Kuznetsov, A.; Chazov, V.; Gorbunov, I.; Zimnukhov, D.; Kuvshinov, D.; Balanutsa, P.; et al. FRB 181016: MASTER optical inspection of the Fast Radio Burst error box. *GCN Circ.* **2018**, 23348, 1.
76. Tyurina, N.; Lipunov, V.; Gorbovskey, E.; Kornilov, V.; Kuznetsov, A.; Chazov, V.; Gorbunov, I.; Zimnukhov, D.; Kuvshinov, D.; Balanutsa, P.; et al. FRB 180714: MASTER optical inspection of the Fast Radio Burst Transient. *GCN Circ.* **2018**, 23010, 1.
77. Aggarwal, K.; Law, C.J.; Burke-Spolaor, S.; Bower, G.; Butler, B.J.; Demorest, P.; Linford, J.; Lazio, T.J.W. VLA/realfast detection of burst from FRB180916.J0158+65. *Astron. Telegr.* **2020**, 13664, 1.
78. Barthelmy, S.D. Observing strategies using GCN. *AIP Conf. Proc.* **1998**, *428*, 129.
79. Barthelmy, S.D.; Cline, T.L.; Butterworth, P. The GRB coordinates network (GCN): A status report. *AIP Conf. Proc.* **1998**, *428*, 99. [\[CrossRef\]](#)
80. Bogovalov, S. Perseus in Sicily: From Black Hole to Cluster Outskirts. In Proceedings of the International Astronomical Union, Noto, Italy, 14–18 May 2018; Volume 342, p. 205.
81. Howell, S.B. *Handbook of CCD Astronomy*, 2nd ed.; Cambridge Observing Handbooks for Research Astronomers, 5; Cambridge University Press: Cambridge, UK, 2006; ISBN 0521852153.
82. Scholz, P.; Cook, A.; Cruces, M.; Hessels, J.W.T.; Kaspi, V.M.; Majid, W.A.; Naidu, A.; Pearlman, A.B.; Spitler, L.G.; Bandura, K.M.; et al. Simultaneous X-ray & Radio Observations of the Repeating Fast Radio Burst FRB 180916.J0158+65. *Astrophys. J.* **2020**, *901*, 165.

83. Scholz, P.; Bogdanov, S.; Hessels, J.W.T.; Lynch, R.S.; Spitler, L.G.; Bassa, C.G.; Bower, G.C.; Burke-Spolaor, S.; Butler, B.J.; Chatterjee, S.; et al. Simultaneous X-ray, Gamma-ray, & Radio Observations of the Repeating Fast Radio Burst FRB 121102. *Astrophys. J.* **2017**, *846*, 80–90.
84. Schlegel, D.J.; Finkbeiner, D.P.; Davis, M. Maps of Dust Infrared Emission for Use in Estimation of Reddening & Cosmic Microwave Background Radiation Foregrounds. *Astrophys. J.* **1998**, *500*, 525.
85. Ade, P.A.R.; Planck Collaboration. Planck 2015 results. *Astron. Astrophys.* **2016**, *594*, A13.
86. Beloborodov, A. Blast Waves from Magnetar Flares & Fast Radio Bursts. *Astrophys. J.* **2020**, *896*, 142.
87. Lipunov, V.; Zhirkov, K.; Kornilov, V.; Gorbovskoy, E.; Gress, O.; Tiurina, N.; Balanutsa, P.; Kuznetsov, A.; Balakin, F.; Vladimirov, V.; et al. SGR 1935+2154: MASTER optical observations. *GCN Circ.* **2020**, 27670, 1.
88. Lipunov, V.; Gorbovskoy, E.; Kornilov, V.; Tyurina, N.; Balanutsa, P.; Kuznetsov, A.; Balakin, F.; Vladimirov, V.; Vlasenko, D.; Gorbunov, I.; et al. Integral GRB200428.61: Global MASTER-Net observations report. *GCN Circ.* **2020**, 27666, 1.
89. Bochenek, C.D.; Ravi, V.; Belov, K.V.; Hallinan, G.; Kocz, J.; Kulkarni, S.R.; McKenna, D.L. A fast radio burst associated with a Galactic magnetar. *Nature* **2020**, *587*, 59–62. [[CrossRef](#)]
90. Zhang, C.F.; Jiang, J.C.; Men, Y.P.; Wang, B.J.; Xu, H.; Xu, J.W.; Niu, C.H.; Zhou, D.J.; Guan, X.; Han, J.L.; et al. A highly polarised radio burst detected from SGR 1935+2154 by FAST. *Astron. Telegr.* **2020**, 13699, 1.
91. Younes, G.; Kouveliotou, C.; Jaodand, A.; Baring, M.G.; van der Horst, A.J.; Harding, A.K.; Hessels, J.W.T.; Gehrels, N.; Gill, R.; Huppenkothen, D.; et al. X-ray and Radio Observations of the Magnetar SGR J1935+2154 during its 2014, 2015, and 2016 Outbursts. *Astrophys. J.* **2017**, *847*, 85. [[CrossRef](#)]
92. De, K.; Ashley, M.C.B.; Andreoni, I.; Kasliwal, M.M.; Soria, R.; Srinivasaragavan, G.P.; Cai, C.; Delacroix, A.; Greffe, T.; Hale, D.; et al. Constraining the X-ray-Infrared Spectral Index of Second-timescale Flares from SGR 1935+2154 with Palomar Gattini-IR. *Astrophys. J. Lett.* **2020**, *901*, L7. [[CrossRef](#)]
93. Chen, G.; Ravi, V.; Lu, W. The multiwavelength counterparts of fast radio bursts. *Astrophys. J.* **2020**, *897*, 146. [[CrossRef](#)]
94. Lyubarsky, Y. Fast radio bursts from reconnection in magnetar magnetosphere. *Astrophys. J.* **2020**, *897*, 1. [[CrossRef](#)]
95. Cordes, J.M.; Wasserman, I. Supergiant pulses from extragalactic neutron stars. *Mon. Not. R. Astron. Soc.* **2016**, *457*, 232. [[CrossRef](#)]
96. Kumar, P.; Lu, W.; Bhattacharya, M. Fast radio burst source properties and curvature radiation model. *Mon. Not. R. Astron. Soc.* **2017**, *468*, 2726. [[CrossRef](#)]
97. Stefanescu, A.; Kanbach, G.; Słowikowska, A.; Greiner, J.; McBreen, S.; Sala, G. Very fast optical flaring from a possible new Galactic magnetar. *Nature* **2008**, *455*, 503–505. [[CrossRef](#)]
98. Dhillon, V.; Marsh, V.S.; Littlefair, S.P.; Copperwheat, C.M.; Hickman, R.D.G.; Kerry, P.; Levan, A.J.; Rea, N.; Savoury, C.D.J.; Tanvir, N.R.; et al. The first observation of optical pulsations from a soft gamma repeater: SGR 0501+4516. *Mon. Not. R. Astron. Soc.* **2011**, *416*, 1. [[CrossRef](#)]
99. Hardy, L.K.; Dhillon, V.S.; Spitler, L.G.; Littlefair, S.P.; Ashley, R.P.; De Cia, A.; Green, M.J.; Jaroenjittichai, P.J.; Keane, E.F.; Kerry, P.; et al. A search for optical bursts from the repeating fast radio burst FRB 121102. *Mon. Not. R. Astron. Soc.* **2017**, *472*, 2800–2807. [[CrossRef](#)]
100. Lin, L.; Zhang, C.F.; Wang, P.; Gao, H.; Guan, X.; Han, J.L.; Jiang, J.C.; Jiang, P.; Lee, K.J.; Li, D.; et al. No pulsed radio emission during a bursting phase of a Galactic magnetar. *Nature* **2020**, *587*, 3–65. [[CrossRef](#)]
101. Acciari, V.A.; Ansoldi, S.; Antonelli, L.A.; Engels, A.A.; Arcaro, C.; Baack, D.; Babić, A.; Banerjee, B.; Bangale, P.; de Almeida, U.B.; et al. Constraining very-high-energy & optical emission from FRB 121102 with the MAGIC telescopes. *Mon. Not. R. Astron. Soc.* **2018**, *481*, 2479–2486.
102. Pilia, M.; Burgay, M.; Possenti, A.; Ridolfi, A.; Gajjar, V.; Corongiu, A.; Perrodin, D.; Bernardi, G.; Naldi, G.; Pupillo, G.; et al. The Lowest-frequency Fast Radio Bursts: Sardinia Radion Telescope Detection of the Periodic FRB 180916 at 328 MHz. *Astrophys. J. Lett.* **2020**, *896*, L40. [[CrossRef](#)]
103. Kilpatrick, C.D.; Burchett, J.N.; Jones, D.O.; Margalit, B.; McMillan, R.; Fong, W.F.; Heintz, K.E.; Tejos, N.; Escorial, A.R. Deep Optical Observations Contemporaneous with Emission from the Periodic FRB 180916.J0158+65. *Astrophys. J.* **2021**, *907*, 1. [[CrossRef](#)]
104. Tendulkar, S.; de Paz, A.G.; Kirichenko, A.Y.; Hessels, J.W.T.; Bhardwaj, M.; Ávila, F.; Bassa, C.; Chawla, P.; Fonseca, E.; Kaspi, V.M.; et al. The 60-pc Environment of FRB 20180916B. *Astrophys. J.* **2020**, *908*, L12. [[CrossRef](#)]
105. Giacomazzo, B.; Perna, R. Formation of Stable Magnetars from Binary Neutron Star Mergers. *Astrophys. J.* **2013**, *771*, L26. [[CrossRef](#)]
106. Piro, L.; Kollmeier, J. Ultrahigh-energy Cosmic Rays from the “En Caul” Birth of Magnetars. *Astrophys. J.* **2016**, *826*, 97. [[CrossRef](#)]
107. Bhattacharya, M.; Kumar, P. Population Modeling of Fast Radio Bursts from Source Properties. *Astrophys. J.* **2020**, *899*, 124. [[CrossRef](#)]
108. Vieyro, F.; Romero, G.E.; Bosch-Ramon, V.; Marcote, B.; del Valle, M.V. A model for the repeating FRB 121102 in the AGN scenario. *Astron. Astrophys.* **2020**, *602*, A64. [[CrossRef](#)]
109. Geng, J.J.; Li, B.; Huang, Y.F. Repeating fast radio bursts from collapses of the crust of a strange star. *Innovation* **2021**, *2*, 100152. [[CrossRef](#)]

-
110. Bhandari, S.; Sadler, E.M.; Xavier Prochaska, J.; Simha, S.; Ryder, S.D.; Marnoch, L.; Bannister, K.W.; Macquart, J.-P.; Flynn, C.; Marnoch, L.; et al. The host galaxies and progenitors of Fast Radio Bursts localized with the Australian Square Kilometre Array Pathfinder. *Astrophys. J. Lett.* **2020**, *895*, L37. [[CrossRef](#)]
 111. Voevodin, V.V.; Antonov, A.S.; Nikitenko, D.A.; Shvets, P.A.; Sobolev, S.I.; Sidorov, I.Y.; Stefanov, K.S.; Voevodin, V.V.; Zhumatiy, S.A. Supercomputer Lomonosov-2: Large Scale, Deep Monitoring and Fine Analytics for the User Community. *Supercomput. Front. Innov.* **2019**, *6*, 4–11. [[CrossRef](#)]